(2)

MTL TR 90-1

AD

QUANTITATIVE MICROSTRUCTURAL ANALYSIS OF UNIDIRECTIONAL CARBON FIBER REINFORCED POLYMER COMPOSITES, PART 1: MICROSTRUCTURAL CHARACTERIZATION OF COMPOSITE CROSS SECTION

JOHN J. RICCA and REBECCA M. JURTA
MATERIALS SCIENCE BRANCH

January 1990

Approved for public release; distribution unlimited.

US ARMY
LABORATORY COMMAND
MATERIALS TECHNOLOGY LABORATORY

U.S. ARMY MATERIALS TECHNOLOGY LABORATORY
Watertown, Massachusetts 02172-0001

The findings in this report are not to be construed as an official Department of the Army position, unless so designated by other authorized documents.

Mention of any trade names or manufacturers in this report shall not be construed as advertising nor as an official indorsement or approval of such products or companies by the United States Government.

DISPOSITION INSTRUCTIONS

Destroy this report when it is no longer needed.
Do not return it to the originator.

UNCLASSIFIED

SECURITY CLASSIFICATION OF THIS PAGE *(When Data Entered)*

REPORT DOCUMENTATION PAGE		READ INSTRUCTIONS BEFORE COMPLETING FORM
1. REPORT NUMBER MTL TR 90-1	2. GOVT ACCESSION NO.	3. RECIPIENT'S CATALOG NUMBER
4. TITLE *(and Subtitle)* QUANTITATIVE MICROSTRUCTURAL ANALYSIS OF UNIDIRECTIONAL CARBON FIBER REINFORCED POLYMER COMPOSITES, PART 1: MICROSTRUCTURAL CHARACTERIZATION OF COMPOSITE CROSS SECTION		5. TYPE OF REPORT & PERIOD COVERED Final Report 6. PERFORMING ORG. REPORT NUMBER
7. AUTHOR(s) John J. Ricca and Rebecca M. Jurta		8. CONTRACT OR GRANT NUMBER(s)
9. PERFORMING ORGANIZATION NAME AND ADDRESS U.S. Army Materials Technology Laboratory Watertown, Massachusetts 02172-0001 SLCMT-EMS		10. PROGRAM ELEMENT, PROJECT, TASK AREA & WORK UNIT NUMBERS D/A Project: 1L162105.AH84
11. CONTROLLING OFFICE NAME AND ADDRESS U.S. Army Laboratory Command 2800 Powder Mill Road Adelphi, Maryland 20783-1145		12. REPORT DATE January 1990 13. NUMBER OF PAGES 34
14. MONITORING AGENCY NAME & ADDRESS *(if different from Controlling Office)*		15. SECURITY CLASS. *(of this report)* Unclassified 15a. DECLASSIFICATION/DOWNGRADING SCHEDULE
16. DISTRIBUTION STATEMENT *(of this Report)* Approved for public release; distribution unlimited.		
17. DISTRIBUTION STATEMENT *(of the abstract entered in Block 20, if different from Report)*		
18. SUPPLEMENTARY NOTES		
19. KEY WORDS *(Continue on reverse side if necessary and identify by block number)* Carbon fiber Polymer composite Laminates Microstructure Image analysis Metallography		
20. ABSTRACT *(Continue on reverse side if necessary and identify by block number)* (SEE REVERSE SIDE)		

DD FORM 1 JAN 73 1473 EDITION OF 1 NOV 65 IS OBSOLETE

UNCLASSIFIED

SECURITY CLASSIFICATION OF THIS PAGE *(When Data Entered)*

Block No. 20

ABSTRACT

Individual axial tensile specimens of AS4/3501-6 and T300/934 unidirectional carbon fiber reinforced polymer composite laminate systems are characterized microstructurally. Fiber volume, fractional fiber volume, fiber uniformity, void volume, and variations in laminate thickness are acquired using automated quantitative image analysis (QIA). The sample preparation methods and QIA system procedures are fully explained. The problems in determining average or batch fiber contents in composite laminates using current methods are discussed. Possible problems in using micrometer thickness data in fiber content calculations are discussed when variations in specimen thickness due to surface contours are present. Variations in microstructure exhibited within a single fabricating company, between several fabricating companies, and between two different fiber-resin systems are demonstrated. Overall, QIA was determined to be a precise means of determining fiber and void contents and uniformity in individual test specimens prior to or after mechanical testing.

CONTENTS

PREFACE

The selection of materials in this study are the unidirectional carbon fiber reinforced polymer (CFRP) composites materials for which a data base was developed as part of the Military Handbook 17 program at the U.S. Army Materials Technology Laboratory (MTL). The purpose of MIL-HDBK-17 is to provide: (1) guidelines for the physical, chemical, and mechanical characterization of composite material systems to be used in aerospace vehicles and structures, (2) compilation of statistically-based mechanical property data for composite material systems used in aerospace industry, and (3) information regarding materials, fabrication, procedures, quality control, design, and analysis.

INTRODUCTION

This is a microstructural characterization study of unidirectional carbon fiber reinforced polymer (CFRP) laminate composites fabricated by eight manufacturers. It was developed to provide the geometrical microstructural characterization of the mechanical test specimens used in the Military Handbook 17[1] program. The findings and recommendations are intended to be helpful in planning future MIL-HDBK-17 studies of CFRP composites.

Part 1 of this microstructural characterization program was undertaken to further the development and evaluation of microstructural characterization using optical quantitative image analysis (QIA) techniques for determining fiber and void content in carbon fiber reinforced polymer composite materials. This report includes: (1) the evaluation of QIA procedures, (2) the materialographic preparation methods, and (3) the macro and microstructural characteristics of the individual processed laminate tensile specimens. The following composite characteristics are determined using QIA methods: laminate thickness, fiber volume, fractional fiber volume, percent voids, total fiber area within a cross section, and qualitative comparison of various types of laminate molded surface contours.

Part 2 is being published as a separate report. Its objectives are: (1) to determine the relationship between the fiber contents of the individual tensile specimens characterized in Part 1 and their corresponding axial tensile strengths, and (2) to present various methods for normalizing ultimate tensile strength of unidirectional CFRP composites.

MATERIAL BACKGROUND

Under the Military Handbook 17 program, prepregs for two different CFRP systems were purchased by MTL and distributed to the companies listed below who volunteered to fabricate laminate panels. The two different CFRP systems used by the various fabricators are:

1. Hercules AS4 Carbon Fiber and 3501-6 Epoxy.

2. Union Carbide T300 Carbon Fiber and Fiberite 934 Hy-E 1034C Epoxy.

Fabricators

AS4/3501-6	T300/934
MTL	MTL
Lockheed - Georgia	Boeing - Seattle
McDonnell Douglas	Lear Fan
Sikorsky Aircraft	Lockheed - California

Conventional autoclave methods were used to fabricate the 12" x 12" seven-ply unidirectional CFRP laminate panels. The samples were mechanically tested for ultimate tensile strength (UTS) at MTL. One-inch-wide tensile specimens were cut from the panels. Fiberglass tabs were adhesively bonded to both surfaces at each end for gripping by tensile tester. The specimens were dry conditioned prior to testing at 50% relative humidity. The tensile test load was applied parallel to the fiber axis, i.e., axial or 0-degree tensile load.

1. Military Handbook 17B Part I: Composite Materials for Aircraft and Aerospace Applications, MIL-HDBK-17B, Volume 1: Guidelines, U.S. Army Materials Technology Laboratory, Draft Copy, September 1987.

The quality assurance certification from Hercules[2] for the CFRP material, AS4/3501-6 prepreg tape, was available. It specifies the manufacturer's tolerances given for fiber density, areal weight of ply, and ply thickness.

QUANTITATIVE IMAGE ANALYSIS: METHODS AND MEASUREMENTS

The quantitative image analysis was performed using a Cambridge Instruments Quantimet 720 System 23 interfaced with a Zeiss Universal Research optical microscope with programmable stage and automatic focusing capabilities. Acquisition of the data is via a Digital Equipment Corporation PDP-11/04 computer. The QIA system is calibrated using an artificial specimen developed and supplied by Cambridge Instruments. (See Appendix A.1 for artificial specimen specifications.)

The artificial specimen is measured prior to each sample measurement. The image analysis measurements are performed by the same operator to reduce variability and provide a greater degree of confidence in the relative aspect of the data.

The QIA measurements were performed on tensile specimens which had been previously tested to failure. The specimens exhibit extensive damage in the gage length section between the fiberglass tabbed ends. However, the fiberglass composite tabs and bonding adhesive prevent the CFRP laminate from being damaged, thus retaining an accurate representation of the composite cross section. This allows for microstructural characterization of the CFRP cross section.

Three specimens from each of the eight fabricated panel types were selected for QIA. The criteria for selection of these three specimens was based on the maximum, minimum, and average load-to-break mechanical test values obtained at MTL for each fabricator.

These cross sections were prepared for QIA measurements using the materialographic procedure described in Appendix A.2. The materialographic preparation was done by the same person using automated metallographic equipment. The diagram, Figure 1a, shows where the sections are cut for mounting, polishing, and analysis. The photomicrograph in Figure 1b is typical of all the materialographic polished cross sections and shows the bonding adhesive and fiberglass composite tabs. The photomicrographs in Figure 2 are the magnified cross-sectional images of the two different fiber types, T300 and AS4.

To provide an assessment of fiber content uniformity along the length of an individual tensile specimen, one section is cut from each of the opposite tabbed ends, thus providing two samples for analysis. The opposite tensile specimen ends are referred to as A and B.

QIA methods are used to measure the following geometrical microstructural aspects of the composite cross section of the unidirectional CFRP tensile specimens: (1) laminate thickness and width, (2) total fiber cross-sectional area, (3) percent fiber in the laminate, and (4) uniformity of fiber distribution within the laminate cross sections.

2. Hercules Incorporated, Aerospace Division, Bacchus Works, Magna, Utah, 84044, 20 October 1982, MTL Purchase Order No. DAAG46-82-M-1474.

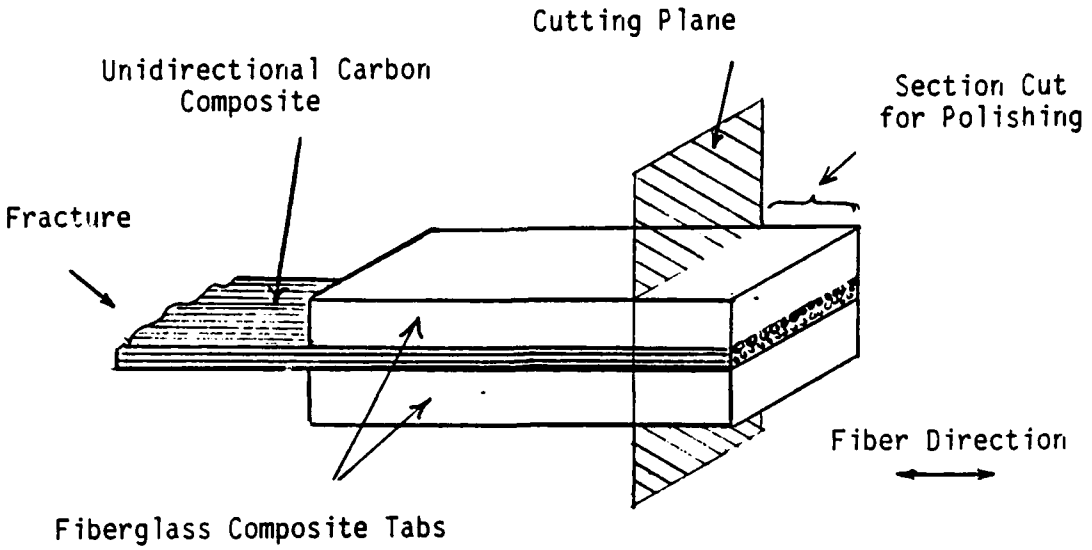

Figure 1a. Portion of tensile specimen cut and polished for QIA analysis.

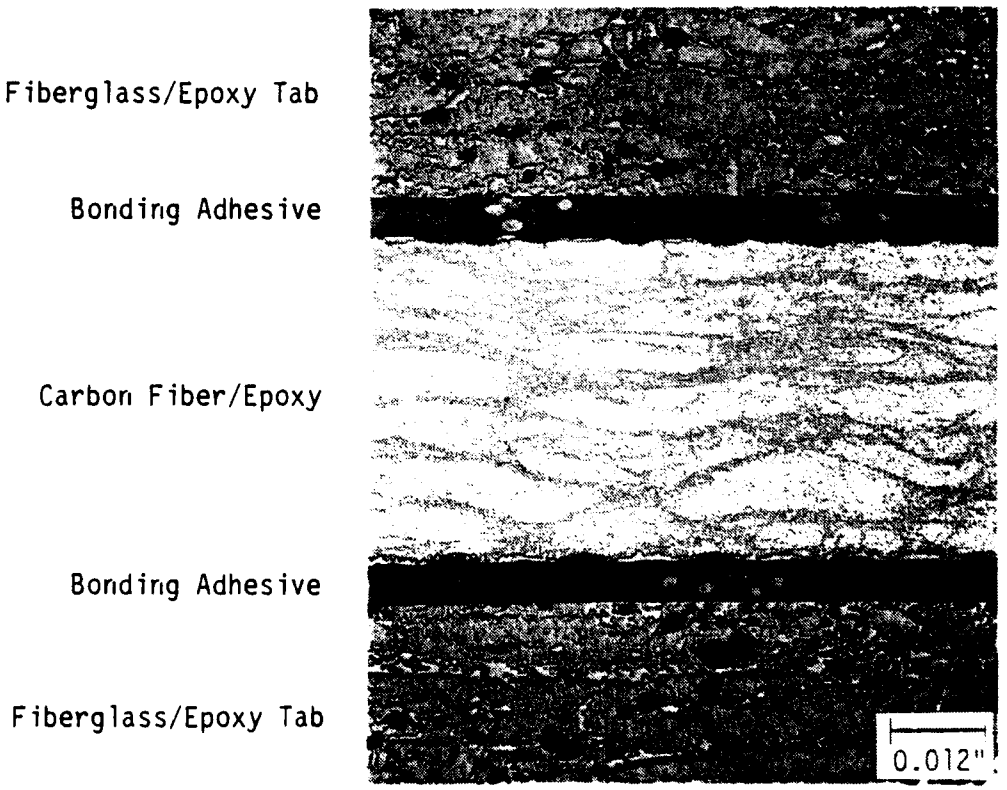

Figure 1b. Photomicrograph of polish cross section of the cut tensile specimen's tabbed end.

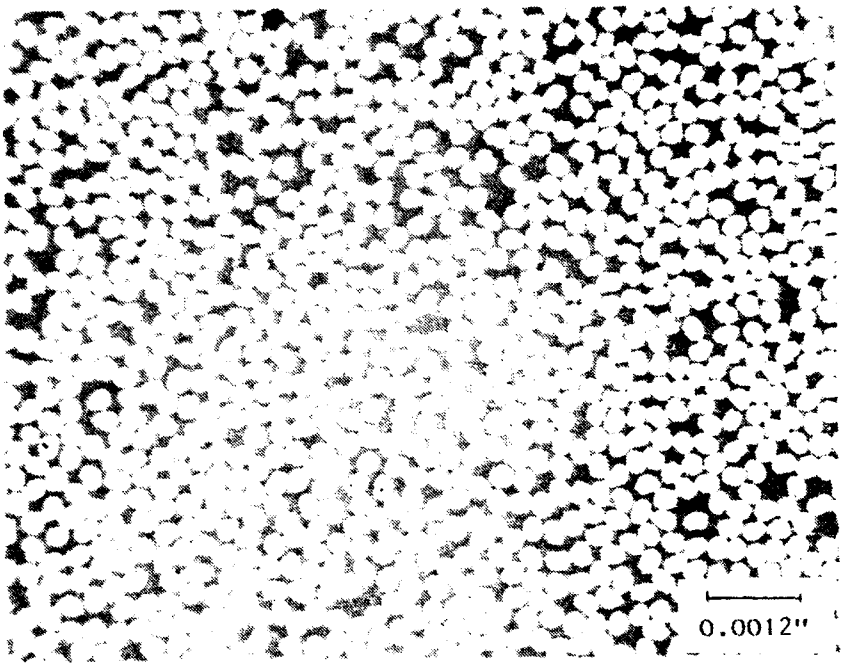

T300: T1, T2, T3, T4

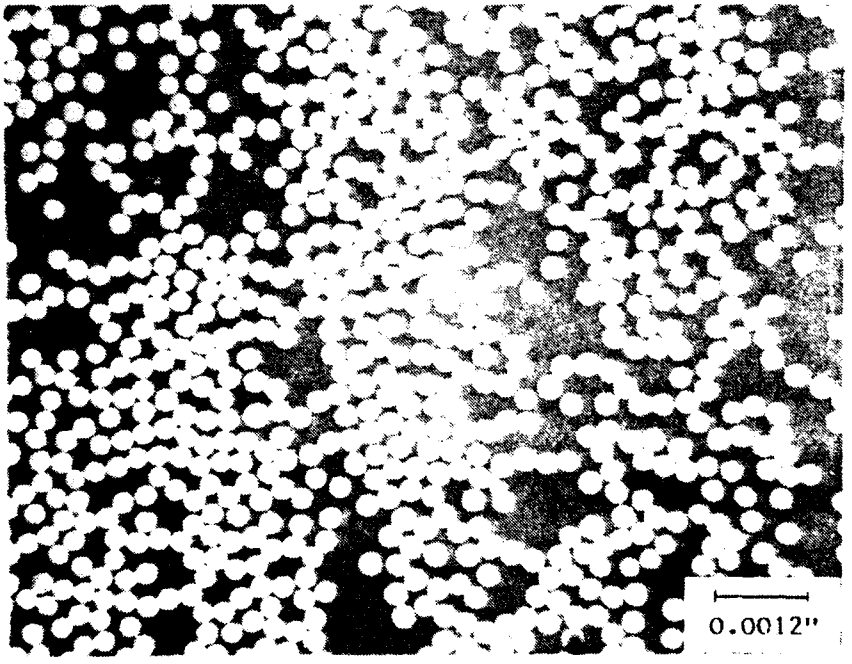

AS4: A1, A2, A3, A4

Figure 2. Optical photomicrographs of polished composite cross sections perpendicular to T300 and AS4 carbon fibers.

Composite Laminate Thickness

The dark field and bright field optical photomicrographs of the laminate cross sections, Figures 3a through 3e, demonstrate the variations of surface contours caused by the different types of release cloth or film used by the various fabricators. For some fabricators, the magnitude of the laminate surface contour variations appear considerable. The standard micrometer methods of measuring laminate thickness, as described in Method 2 below, do not allow or compensate for surface contour irregularity. Method 1, discussed below, is introduced as a more accurate measurement of laminate thickness, thus providing greater accuracy in the calculation of the tensile specimen's cross-sectional area.

Quantitative image analysis technology has the capability of directly measuring the overall composite cross-sectional area. However, because of the time needed to develop special specimen preparation methods for edge enhancement, it was not included in this study.

Method 1

Thickness measurements are acquired from the polished cross sections using the X-Y precision stage measuring capability and the Zeiss microscope. The illustration in Figure 4 depicts an exaggerated surface contour of a laminate cross section.

A maximum thickness (t_m) is obtained by measuring the distance between the contour peaks on one surface to the peaks on the opposite surface of the laminate (see Figure 4). The minimum laminate thickness (t_s) is obtained by measuring between the lowest point or valley of contours on one surface to the valley on the opposite surface of the laminate (see Figure 4); thus, an upper and lower bound for the thickness is determined. The average thickness (t_1) is determined using Equation 1.

$$t_1 = (t_m + t_s)/2 \qquad (1)$$

The width (W) for the tensile specimens is also determined using the X-Y stage measuring system. The X-Y stage precision is $\pm 2.5\ \mu m$ or ± 0.0001 inches.

Method 2

In this method, a conventional hand held, flat anvil, screw micrometer is used to measure laminate thickness (t_2). The two opposite anvil faces of the micrometer span the peaks of the surface contours. This is similar to the QIA procedure for making the upper bound thickness (t_m) measurements in Method 1. Another micrometer type, such as ball ended, would be an improvement over the flat anvil type.[3]

The QIA thickness data (t_1) is considered to be the more accurate representation of the average composite thickness since surface contours exist. The importance of laminate thickness accuracy will become apparent when the methods of determining fiber volume content are discussed later.

3. KOWALSKI, I. M. *Determining the Transverse Modulus of Carbon Fibers.* SAMPE Journal, July/August 1986, p. 39.

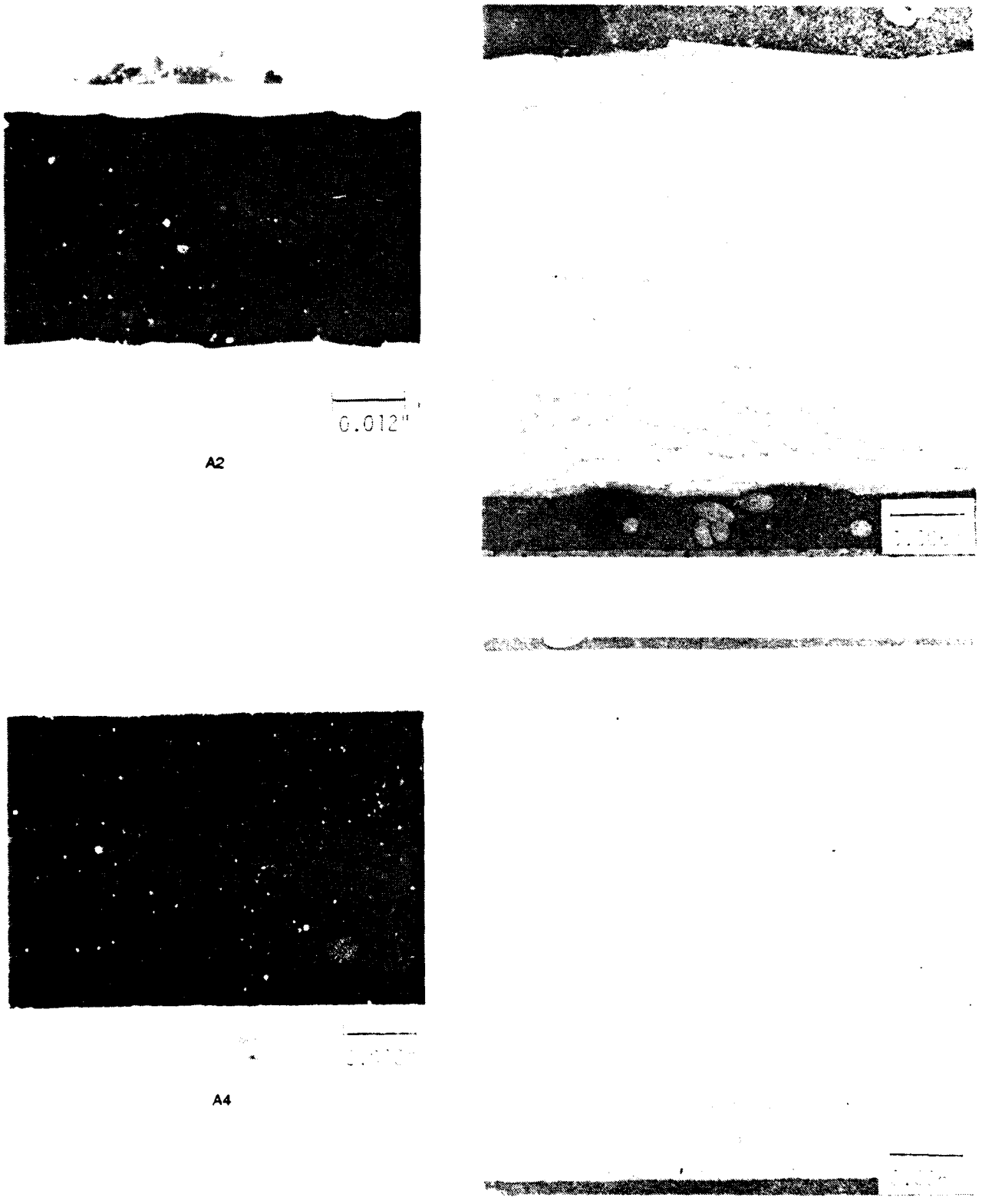

Figure 3a. Dark field and bright field optical photomicrographs of polished tensile specimen cross sections showing molded surface contours and fiber/resin uniformity.

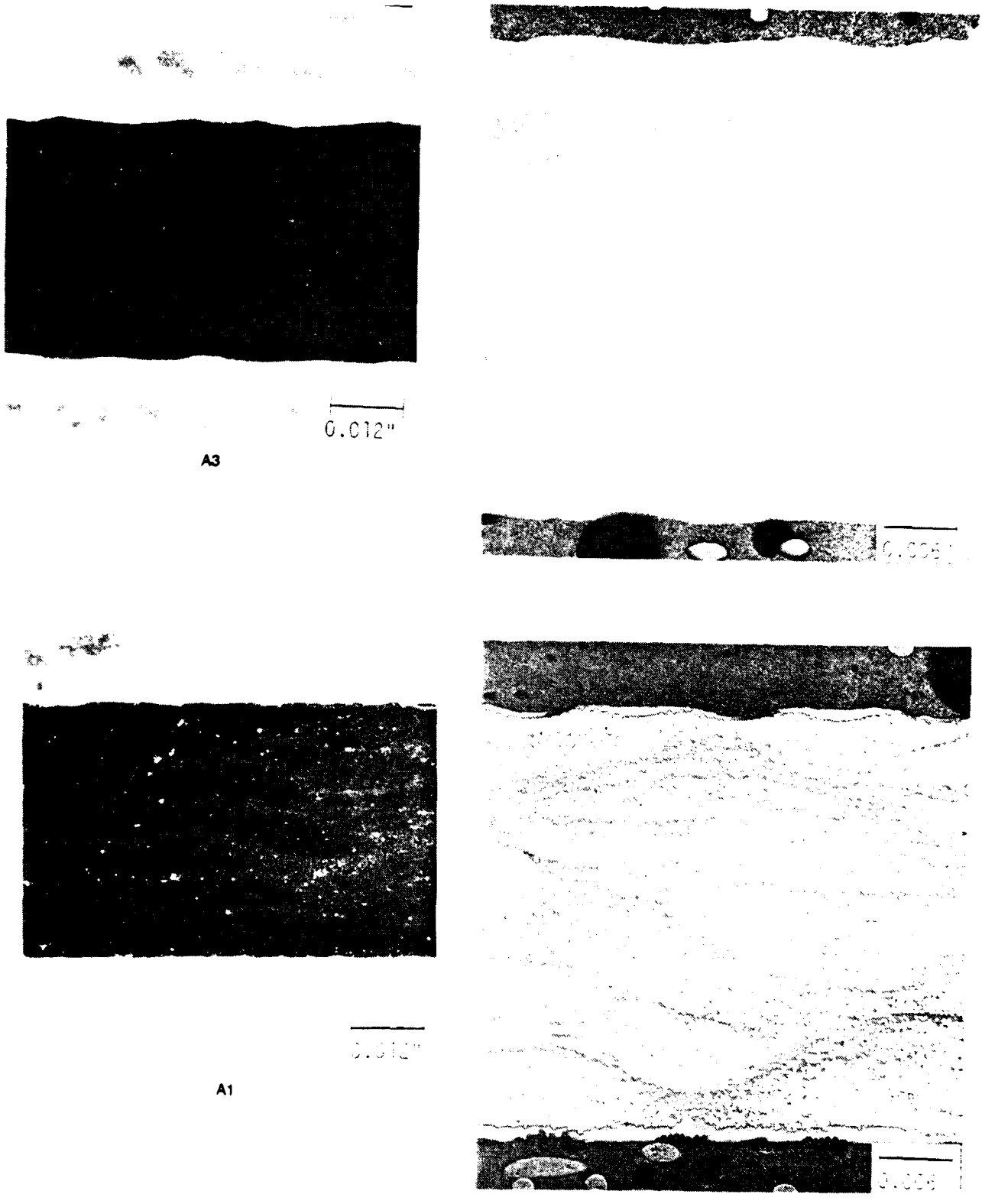

Figure 3b. Dark field and bright field optical photomicrographs of polished tensile specimen cross sections showing molded surface contours and fiber/resin uniformity.

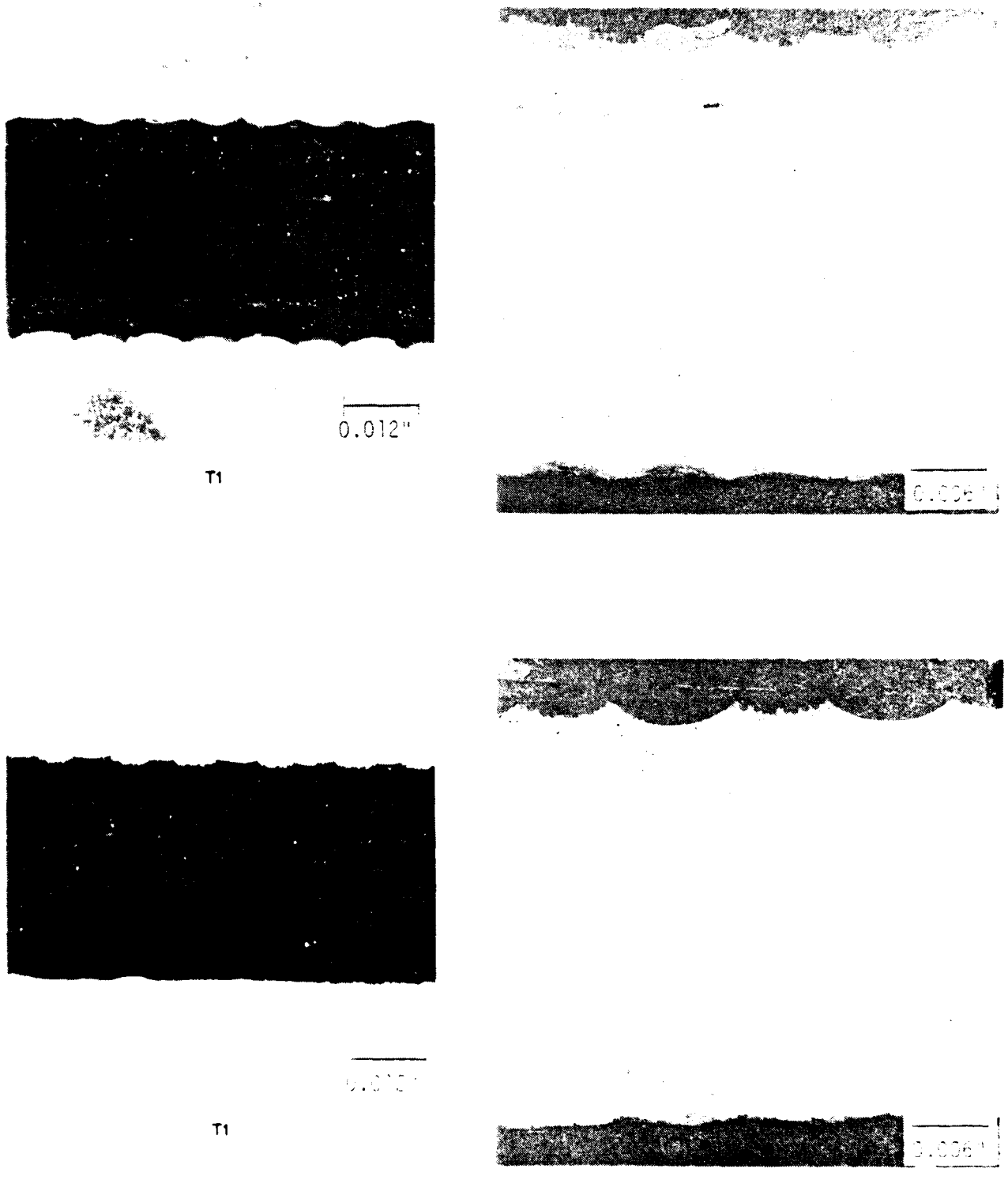

Figure 3c. Dark field and bright field optical photomicrographs of polished tensile specimen cross sections showing molded surface contours and fiber/resin uniformity.

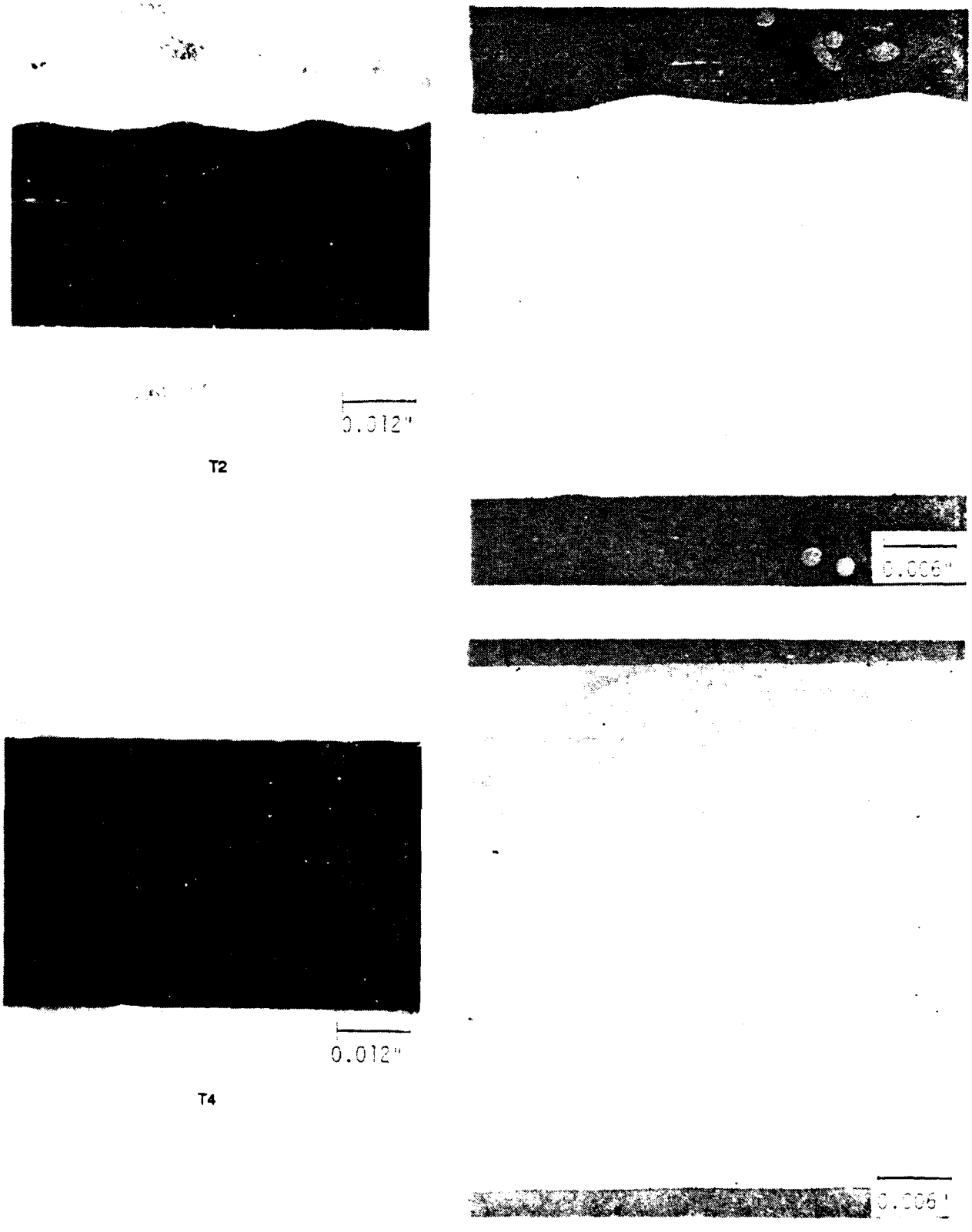

Figure 3d. Dark field and bright field optical photomicrographs of polished tensile specimen cross sections showing molded surface contours and fiber/resin uniformity.

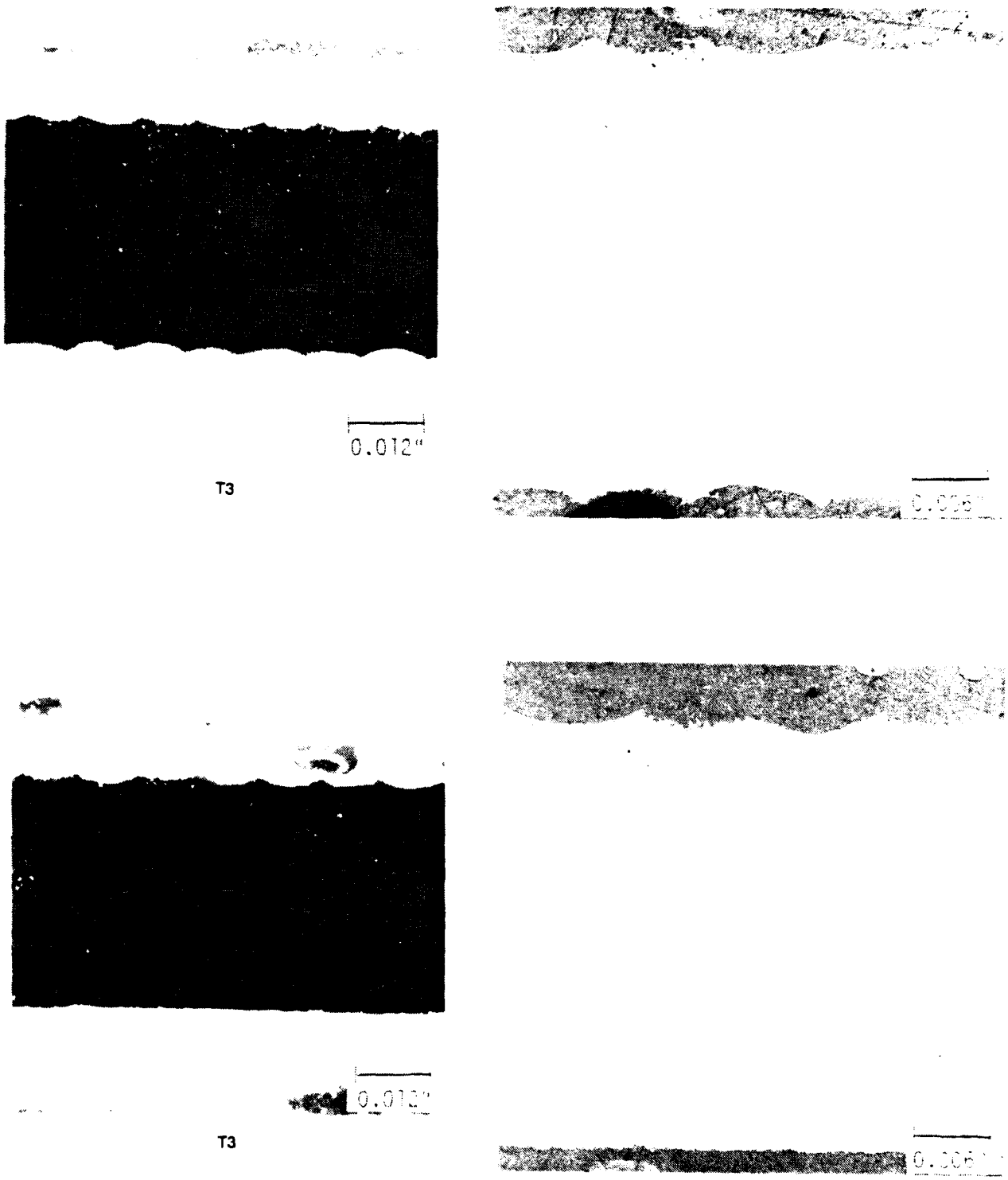

Figure 3e. Dark field and bright field optical photomicrographs of polished tensile specimen cross sections showing molded surface contours and fiber/resin uniformity.

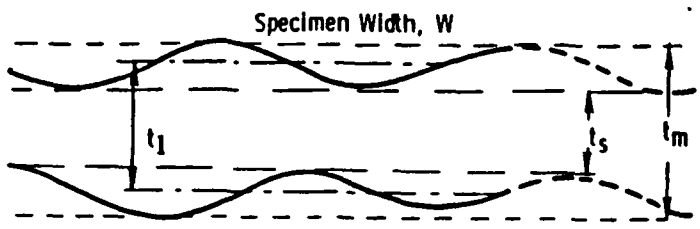

t_1 = average thickness $\quad t_1 = (t_s + t_m)/2$

t_s = minimum thickness

t_m = maximum thickness

Figure 4. Illustration of molded surface contours and thickness variations.

Total Cross-Sectional Fiber Area (A_{f1}): Method 1

The Quantimet optical QIA system is used to measure the average total fiber cross-sectional area (A_{f1}) of the tensile specimen. For unidirectional fiber composites, the fiber cross-sectional area is numerically equivalent to the fiber volume.[4] The QIA measurement procedure is as follows.

The polished specimens are leveled and aligned parallel to X direction of the automatic scanning microscope stage. Each specimen is fixed to a metal microscope slide using a soft clay; secure but removable. The microscope is set at 200X and the image is projected on the Quantimet CRT monitor via a Vidicon camera. The actual Quantimet measurement magnification is 435X. The carbon fibers in the polymer matrix are electronically "detected" or differentiated by their optical contrast difference.

The entire composite cross section, typically 0.0400 ±0.0050 square inches, is scanned using a programmed X-Y pattern. Each field of view in the matrix pattern is referred to as a measuring frame or simply a "frame." Each frame is approximately 0.0177 x 0.0138 inches and programmed to butt with each adjoining frame in a matrix array. The butting precision of the frame is ±2.5 μm or ±0.0001 inches. The total number of frames needed to scan an entire composite sample cross section varies from 171 to 232.

The Quantimet PDP-11/04 computer is programmed to sum the fiber area measurements from all the frames scanned in the entire cross section. This provides the total fiber area in each tensile specimen cross section. The total fiber area measurement is repeated three times for each tensile specimen and averaged to determined the average total cross-sectional fiber area (A_{f1}).

4. UNDERWOOD, E. E. Quantitative Stereology. Addison-Wesley, MA, 1970, p. 27.

Percent Cross-Sectional Fiber Area ($\%A_{f1}$) and ($\%A_{f2}$)

Two different methods are used to determine the percent fiber area in each specimen cross section. Method 1 involves calculating the percent fiber using the QIA measurements of total fiber cross-sectional area and specimen cross-sectional area. In Method 2, a direct measurement of percent fiber is obtained using the Quantimet. In either case, fiber area fraction is equivalent to fiber volume fraction.[3]

Method 1 ($\%A_{f1}$)

The percent fiber area of the tensile specimen ($\%A_{f1}$) is calculated using the total fiber cross-sectional area measured using QIA (A_{f1}) divided by its cross-sectional area (A_Q). A_Q is the product of the width (W) and thickness (t_1) of the individual tensile specimen, which were both measured using the QIA X-Y stage. The percent fiber is calculated using Equation 2.

$$\%A_{f1} = [A_{f1}/A_Q]\ (100) = [A_{f1}/(t_1)(W)]\ (100) \tag{2}$$

Method 2 ($\%A_{f2}$)

The average percent fiber area ($\%A_{f2}$) is obtained by direct QIA measurement. The Quantimet is programmed to measure the fiber area within each frame and divide it by the frame area, i.e., the percent fiber area for each frame ($\%A_{f_i}$). The average percent fiber area ($\%A_{f2}$) for each specimen is automatically calculated by the computer by summing the percent fiber area measurement for each individual frame divided by the number of frames (N) (see Equation 3).

$$\%A_{f2} = \sum_{i=1}^{N} \%A_{f_i}/N \tag{3}$$

A typical histogram distribution of percent fiber area ($\%A_{f_i}$) versus number of frames measured (N) is shown in Figure 5. The computer also provides statistical information: mean, minimum, maximum, median, and standard deviation of the average percent fiber for each specimen.

The Quantimet scanned and measured approximately 60% to 90% of the total cross-sectional area of each of the individual specimens. The entire specimen cross section could not be scanned while performing the QIA $\%A_{f2}$ measurements for two reasons. First, the irregular molded surface contours (as seen in the dark field photographs, Figures 3a through 3e, left photo) in the composite cross section had to be excluded from the QIA measurement due to the square measuring frame of the Quantimet system. Secondly, some of the composite cross section was excluded due to slight nonparallel sample alignment with respect to the microscope stage scanning array.

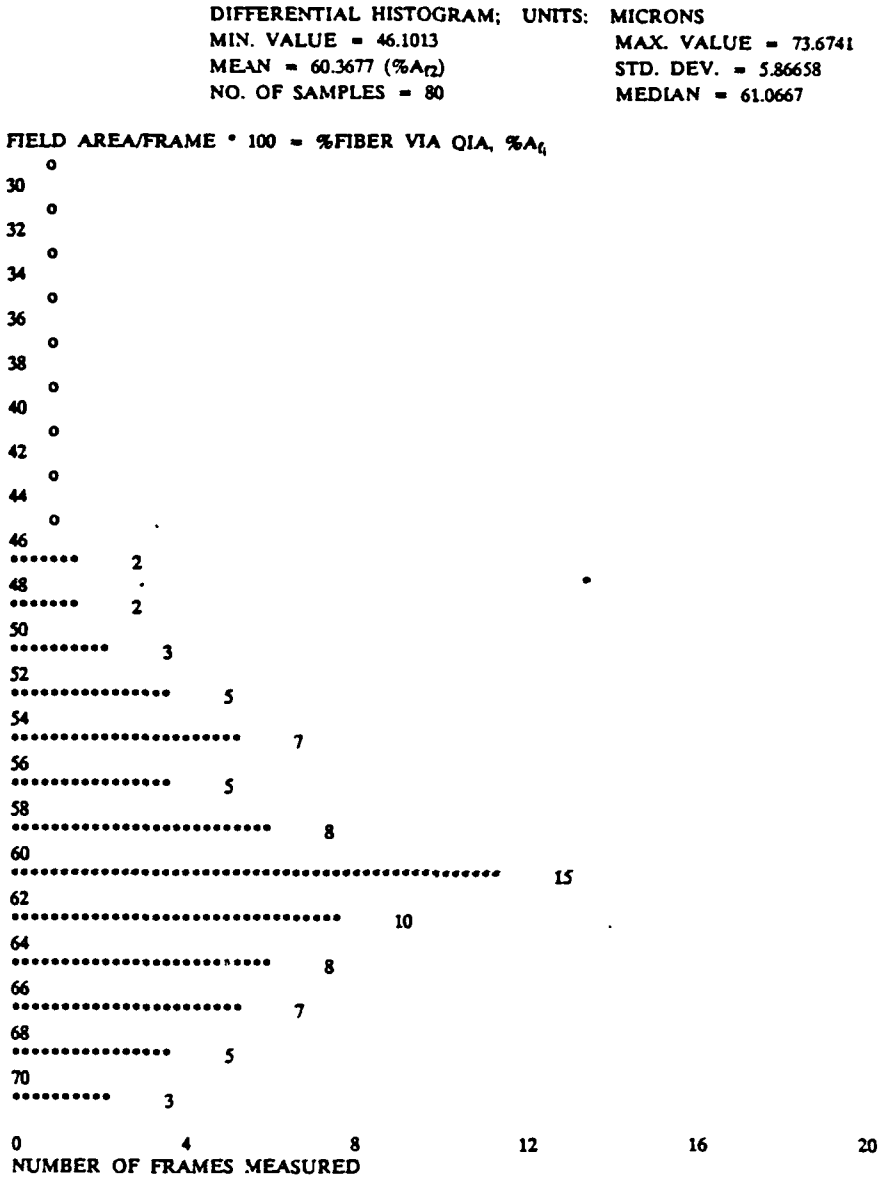

Figure 5. Typical specimen histogram for percent fiber area, $\%A_{f2}$.

Total Cross-Sectional Fiber Area (A_{f2}): Method 2

Method 2 presents an alternative procedure to that previously described in Method 1 (A_{f1}) for determining the total cross-sectional fiber area in an individual tensile specimen. In Method 2, the total fiber area (A_{f2}) is calculated for a tensile specimen using the corresponding value of $\%A_{f2}$, and the overall cross-sectional area (A_Q) (see Equation 4). A_Q is the product of the specimen width (W) and the thickness (t_1) as measured using QIA methods.

$$A_{f2} = (\%A_{f2})(W)(t_1)/100 = (\%A_{f2})(A_Q)/100 \quad (4)$$

Fiber Area Per Unit Width (A_f/W)

The fiber area per unit width of composite laminate is used to facilitate the estimation of fiber content in test specimens of varying widths and provide a useful parameter for characterizing and comparing CFRP laminates. Typically, this is calculated from the manufacturer's batch specifications.[2] Whereas, QIA methods are used on the processed laminate and provide a measure of the fiber area per unit width variability in a panel cross section. Below are two QIA methods used for determining the total fiber area per unit width for each tensile specimen.

Method 1 $(A_f/W)_1$

Fiber area per unit width of composite $(A_f/W)_1$ is calculated using the average total fiber area determined from direct QIA measurements (A_{f1}) and the sample width (W) (see Equation 5).

$$(A_f/W)_1 = A_{f1}/W \tag{5}$$

Method 2 $(A_f/W)_2$

Fiber area per unit width of composite $(A_f/W)_2$ is calculated using the percent fiber area from direct QIA measurements ($\%A_{f2}$) and the average thickness obtained from the QIA method (t_1) (see Equation 6), which is equivalent to A_{f2} (see Equation 4) divided by the sample width (W).

$$(A_f/W)_2 = (\%A_{f2})(t_1) = A_{f2}/W \tag{6}$$

Uniformity of Fiber Within a Composite Cross Section

As seen in the bright field photomicrographs in Figures 3a through 3e, right photo, the carbon filaments are not uniformly distributed throughout the specimen cross section. The percent fiber area histogram (see Figure 5) provides a graphical representation of the percent fiber variation in the scanned cross section. The corresponding standard deviation of the percent fiber area is a quantitative indicator of how much the percent fiber varies in a cross section.

Standard deviation is affected by the image analyzer magnification used in performing the percentage fiber area measurements.[5] In this study, all the $\%A_{f2}$ measurements were performed at the same magnification, 435X, making it possible to compare the standard deviation variations between specimens; thus, the standard deviation could be used to estimate the degree of fiber uniformity within the scanned portion of the cross section.

In some cases, the specimens exhibit excess resin regions along the molded surfaces. These regions are usually excluded from this uniformity measurement because of the Quantimet square boundary frame and sample alignment limitations cited in the previous percent

5. VANDER VOORT, G. *Influence of Magnification on Feature Specific Image Analysis Measurements.* Metallography, v. 21, 1988, p. 327-345.

fiber area section. The original photomicrographs (see Figures 3a through 3e) show which laminates exhibit this excess resin characteristic, although the reproduction of the images may make this difficult to detect.

TABULATED RESULTS

The QIA data for each fabricator is tabulated in Tables 1 through 8. A and B refer to the opposite ends of the particular tensile specimen analyzed. Identification of the column headings are listed below. Conversion factors and additional terms are listed for quick reference. English and metric units are used throughout the results section.

SAMPLE NUMBER: A and B refer to the opposite ends of the individual tensile specimen.

THICKNESS (t_1), μm: Average of 5 thickness measurements along the width in microns with ± referring to the maximum and minimum thickness of the surface contour (see Equation 1).

WIDTH (W), μm: QIA tensile specimen width in microns.

SPECIMEN AREA (A_Q), μm^2: Composite cross-sectional area calculated from the QIA measurements of average thickness and width (see Equation 2) in square microns.

FIBER AREA (A_{f1}), ± STD DEV, μm^2: Average of the three repeated QIA total cross-sectional fiber area measurements in square microns.

%FIBER AREA (%A_{f1}): Average percent fiber cross-sectional area in composite specimen calculated using total fiber area via QIA, A_{f1}, divided by the composite cross-sectional area of specimen, A_Q x 100 (see Equation 2).

%FIBER (%A_{f2}) ± STD DEV: Average percent fiber with ± the standard deviation determined from direct measurement QIA (see Equation 3). The percentage of the sample cross-sectional area actually scanned for this measurement is shown in parentheses.

Conversion Factors:

μm = micrometers or microns; 1 μm = 3.937 x 10^{-5} inches

μm^2 = square micrometers or square microns; 1 μm^2 = 1.55 x 10^{-9} inches

Other Terms in This Report:

t_2: Micrometer method thickness, micrometers or inches

$(A_f/W)_1$: Average fiber area per unit width calculated from (A_{f1} via QIA)/(sample width, W), $in.^2/in.$ (see Equation 5)

$(A_f/W)_2$: Average fiber area per unit width calculated from (%A_{f2})(t_1), $in.^2/in.$ (see Equation 6)

A_{f2}: Calculated total cross-sectional fiber area from (%A_{f2})(A_Q)/100, $in.^2$ or μm^2 (see Equation 4)

Table 1. QIA DATA FOR A1 TENSILE SPECIMENS

Sample Number	Thickness t_1, μm	Width W, μm	Specimen Area A_Q, μm^2	Fiber Area A_{f1}, μm^2	%Fiber Area $\%A_{f1}$	%Fiber, $\%A_{f2}$ ± Std. Dev.
A1 A-3-1-9	1024 ±8	25,365	2.597376×10^7	1.599984×10^7	61.6	61.6 ±6.0 (90%)
A1 B-3-1-9	1080 ±16	25,493	2.753244×10^7	1.591375×10^7	57.8	57.8 ±5.7 (85%)
A1 A-3-3-9	1093 ±8	25,435	2.7800455×10^7	1.609646×10^7	57.9	57.9 ±5.4 (91%)
A1 B-3-3-9	1076 ±15	25,455	2.738958×10^7	1.615985×10^7	59.0	59.0 ±5.5 (92%)
A1 A-3-3-10	947 ±10	25,385	2.4039595×10^7	1.500071×10^7	62.4	62.4 ±5.0 (70%)
A1 B-3-3-10	949 ±22	25,425	2.4128325×10^7	1.486305×10^7	61.6	61.6 ±5.0 (70%)

Table 2. QIA DATA FOR A2 TENSILE SPECIMENS

Sample Number	Thickness t_1, μm	Width W, μm	Specimen Area A_Q, μm^2	Fiber Area, A_{f1} ± Std. Dev., μm^2	%Fiber Area $\%A_{f1}$	%Fiber, $\%A_{f2}$ ± Std. Dev.
A2 3-A-48	840 ±46	25,320	2.12688×10^7	1.4775411×10^7 $\pm 8.2978035 \times 10^4$	69.4	65.2 ±6.9 (76%) (0.53% Void)
A2 3-B-48	841 ±31	25,410	2.136981×10^7	1.4514403×10^7 $\pm 24.515106 \times 10^4$	67.9	67.0 ±4.7 (77%) (0.16% Void)
A2 10-A-39	954 ±12	25,415	2.424591×10^7	1.665913×10^7 $\pm 21.572616 \times 10^4$	68.7	66.4 ±3.6 (73%)
A2 10-B-39	997 ±12	25,400	2.53238×10^7	1.6518028×10^7 $\pm 17.628767 \times 10^4$	65.2	64.7 ±3.5 (71%)
A2 3-A-40	972 ±15	25,355	2.464506×10^7	1.5860251×10^7 $\pm 4.22236 \times 10^4$	64.4	64.0 ±4.7 (90%)
A2 3-B-40						

Table 3. QIA DATA FOR A3 TENSILE SPECIMENS

Sample Number	Thickness t_1, μm	Width W, μm	Specimen Area A_Q, μm^2	Fiber Area, A_{f1} ± Std. Dev., μm^2	%Fiber Area $\%A_{f1}$	%Fiber, $\%A_{f2}$ ± Std. Dev.
A3 10-A-69-34		25,435				62.2 ±4.0 (36%)
A3 10-B-69-34	1035 ±9	25,460	2.63511×10^7	1.601492×10^7 $\pm 0.50513266 \times 10^4$	60.8	59.4 ±5.3 (36%)
A3 11-A-69-38	1043 ±16	25,480	2.657564×10^7	1.542676×10^7 $\pm 24.06807 \times 10^4$	58.0	58.2 ±5.1 (61%)
A3 11-B-69-38	987 ±18	25,435	2.5104345×10^7	1.5811341×10^7 $\pm 21.934316 \times 10^4$	63.0	61.8 ±3.9 (67%)
A3 11-A-69-36	1029 ±13	25,435	2.6172615×10^7	1.588989×10^7 $\pm 4.8505353 \times 10^4$	60.7	59.0 ±4.8 (68%)
A3 11-B-69-36	1023 ±5	25,480	2.606604×10^7	1.6309363×10^7 $\pm 1.4493689 \times 10^4$	62.6	59.9 ±5.2 (64%)

Table 4. QIA DATA FOR A4 TENSILE SPECIMENS

Sample Number	Thickness t_1, μm	Width W, μm	Specimen Area A_Q, μm^2	Fiber Area, A_{f1} ± Std. Dev., μm^2	%Fiber Area $\%A_{f1}$	%Fiber, $\%A_{f2}$ ± Std. Dev.
A4-13-AS4 4-11-A	1254 ±5	25,392	3.1841568×10^7	1.6689717×10^7 $\pm 30.378 \times 10^4$	52.4	49.1 ±5.8 (60%)
A4-13-AS4 4-11-B	1140 ±10	25,495	2.90643×10^7	1.6398425×10^7 $\pm 9.80845 \times 10^4$	56.4	53.1 ±5.9 (88%)
A4-3-AS4 4-8-A	Fractured into Tabbed Area					
A4-3-AS4 4-8-B	1200 ±5	25,883	3.10586×10^7	1.5226695×10^7 $\pm 2.55286 \times 10^4$	49.0	50.2 ±7.0 (79%)
A4-7-AS4 4-10-A	1290 ±6	25,375	3.273375×10^7	1.7138533×10^7 $\pm 2.47993 \times 10^4$	52.4	50.6 ±6.5 (80%)
A4-7-AS4 4-10-B	1316 ±16	25,395	3.341982×10^7			49.8 ±6.1 (74%)

Table 5. QIA DATA FOR T1 TENSILE SPECIMENS

Sample Number	Thickness t_1, μm	Width W, μm	Specimen Area A_Q, μm^2	Fiber Area, A_{f1} ± Std. Dev., μm^2	%Fiber Area $\%A_{f1}$	%Fiber, $\%A_{f2}$ ± Std. Dev.
T1 4-A	913 ±18	25,500	2.32815×10^7	1.5939583×10^7 $\pm 3.3061714 \times 10^4$	68.5	69.5 ±2.1 (75%)
T1 4-B	934 ±18	25,645	2.395243×10^7	1.573349×10^7 $\pm 5.9692932 \times 10^4$	65.7	66.7 ±3.8 (75%)
T1 61-A	866 ±30	25,580	2.215228×10^7	1.4230193×10^7 $\pm 0.37765107 \times 10^4$	64.2	67.1 ±2.1 (81%)
T1 61-B	877 ±42	25,570	2.242489×10^7	1.424309×10^7 $\pm 3.5305949 \times 10^4$	63.5	66.7 ±2.1 (80%)
T1 91-A	906 ±24	25,560	2.315736×10^7	1.5058233×10^7 $\pm 1.2026605 \times 10^4$	65.0	67.1 ±2.5 (77%)
T1 91-B	887 ±21	25,485	2.2605195×10^7	1.4695503×10^7 $\pm 1.4495807 \times 10^4$	65.0	65.8 ±2.3 (77%)

Table 6. QIA DATA FOR T2 TENSILE SPECIMENS

Sample Number	Thickness t_1, μm	Width W, μm	Specimen Area A_Q, μm^2	Fiber Area, A_{f1} ± Std. Dev., μm^2	%Fiber Area $\%A_{f1}$	%Fiber, $\%A_{f2}$ ± Std. Dev.
T2 4-A	850 ±26	25,600	2.176×10^7	1.5484532×10^7 $\pm 7.7876123 \times 10^4$	71.2	69.4 ±1.9 (82%)
T2 4-B	853 ±18	25,545	2.1789685×10^7	1.5379637×10^7 $\pm 4.7576434 \times 10^4$	70.6	69.4 ±2.4 (82%)
T2 13-A	889 ±11	25,600	2.27584×10^7	1.5781533×10^7 $\pm 1.4406783 \times 10^4$	69.3	69.5 ±2.4 (77%)
T2 13-B	881 ±10	25,560	2.251836×10^7	1.5550973×10^7 $\pm 2.3064055 \times 10^4$	69.1	69.4 ±2.5 (78%)
T2 58-A	879 ±32	25,550	2.245845×10^7	1.5478457×10^7 $\pm 6.3693069 \times 10^4$	68.9	68.2 ±2.7 (78%)
T2 58-B	883 ±14	25,535	2.2547405×10^7	1.5816667×10^7 $\pm 9.110182 \times 10^4$	70.1	69.0 ±2.2 (78%)

Table 7. QIA DATA FOR T3 TENSILE SPECIMENS

Sample Number	Thickness t_1, μm	Width W, μm	Specimen Area A_Q, μm^2	Fiber Area, A_{f1} ± Std. Dev., μm^2	%Fiber Area $\%A_{f1}$	%Fiber, $\%A_{f2}$ ± Std. Dev.
T3 15-A	952 ±33	25,580	2.435216×10^7	1.5877558×10^7 $\pm 3.5006153 \times 10^4$	65.2	67.3 ±2.8 (69%)
T3 15-B						
T3 12-A	886 ±18	25,500	2.2593×10^7	1.4803268×10^7 $\pm 2.9284814 \times 10^4$	65.5	66.6 ±3.3 (74%)
T3 12-B						
T3 13-A	944 ±29	25,580	2.414752×10^7	1.5790617×10^7 $\pm 4.560764 \times 10^4$	65.4	65.5 ±2.7 (69%)
T3 13-B	936 ±17	25,555	2.391948×10^7	1.541671×10^7 $\pm 4.938518 \times 10^4$	64.5	65.4 ±2.2 (71%)

Table 8. QIA DATA FOR T4 TENSILE SPECIMENS

Sample Number	Thickness t_1, μm	Width W, μm	Specimen Area A_Q, μm^2	Fiber Area, A_{f1} ± Std. Dev., μm^2	%Fiber Area $\%A_{f1}$	%Fiber, $\%A_{f2}$ ± Std. Dev.
T4-A5-42-3	1139 ±2	25,490	2.903311×10^7	1.5576843×10^7 $\pm 4.859 \times 10^4$	53.6	52.2 ±2.7 (90%)
T4-B5-46-4	963 ±4	25,500	2.45565×10^7	1.5638257×10^7 $\pm 4.970365 \times 10^4$	63.7	63.6 ±3.3 (71%)
T4-B5-50-2	1138 ±1	25,465	2.897917×10^7	1.4880847×10^7 $\pm 2.48476 \times 10^4$	51.4	50.1 ±4.7 (91%)

DISCUSSION OF RESULTS

Surface Contour and Laminate Thickness

In Figures 3a through 3e, two photomicrographs are used to show typical cross-sectional views for each specimen fabricator. Dark field, incident light illumination at 40X magnification emphasizes the surface contours. Bright field, incident light illumination at 80X shows general fiber distribution within the polymer matrix and some additional surface geometry detail. As evident in the photomicrographs shown, the surface contours of the processed laminate vary considerably between fabricators and, in two cases (see Figures 3a and 3e), within a fabricator. These surface contour variations are the result of different types of mold release film or different styles of mold release bleeder fabric used in the autoclave panel fabrication process. The A4 and T4 samples used mold release film rather than bleeder cloth and show smooth edges with excess resin (see Figures 3a and 3e).

Table 9 lists average fabricator thickness of the laminate, the difference in the maximum and minimum thickness (Δt), and the percentage ratio of Δt to the average thickness (t_1). This percent ratio ($\%\Delta T$) attempts to place a quantitative value on the sample surface contour variations relative to the average laminate thickness. The $\%\Delta T$ ranges from 0% to 6% for the different fabricators.

Table 9. LAMINATE CFRP SAMPLE THICKNESS VARIABILITY DUE TO SURFACE CONTOUR VARIATIONS CAUSED BY AUTOCLAVE MOULD RELEASE CLOTH AND FILM

AS4/3501-6				T300/934			
MFG	t_1, Inches	Δt, Inches	%ΔT	MFG	t_1, Inches	Δt, Inches	%ΔT
A1	0.04048	0.00111	2.7	T1	0.03532	0.00192	5.4
A2	0.03625	0.00174	4.8	T2	0.03435	0.00174	5.1
A3	0.04029	0.00114	2.8	T3	0.03659	0.00271	5.9
A4	0.04882	0.00080	1.6	T4	0.04021	-0-	—

t_m = maximum thickness

t_s = minimum thickness

t_1 = average thickness

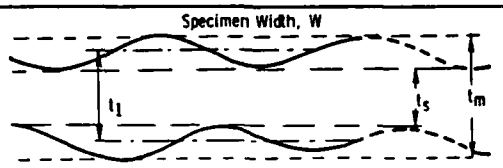

$t_1 = (t_m + t_s)/2$

$\Delta t = t_m - t_s$

$\%\Delta T = (\Delta t/t_1)\ 100$

An example of a somewhat large average surface contour variation is shown in Table 9 for manufacturer T3. The laminate has an average variation (Δt) of 0.0022 inches and an average laminate thickness (t_1) of 0.0366 inches. Thus, the overall contour variation (Δt) is approximately 6% of the laminate thickness. This is larger than the typical specified ±1% accuracy associated with micrometer measurements. The above example demonstrates the need for further investigation of more accurate methods of measuring laminate thickness where contour variations are appreciable.

In Figure 6, the tensile specimen thickness determined using QIA techniques (t_1) is plotted for each fabricator. This graphically illustrates the thickness variation within a manufacturer and between the different manufacturers. Since the widths of the tensile specimens are relatively uniform throughout *all the tensile specimens, 1.0000 ±0.0050 inches, this* figure is indicative of the relative variation in the composite cross-sectional area of the tensile specimens.

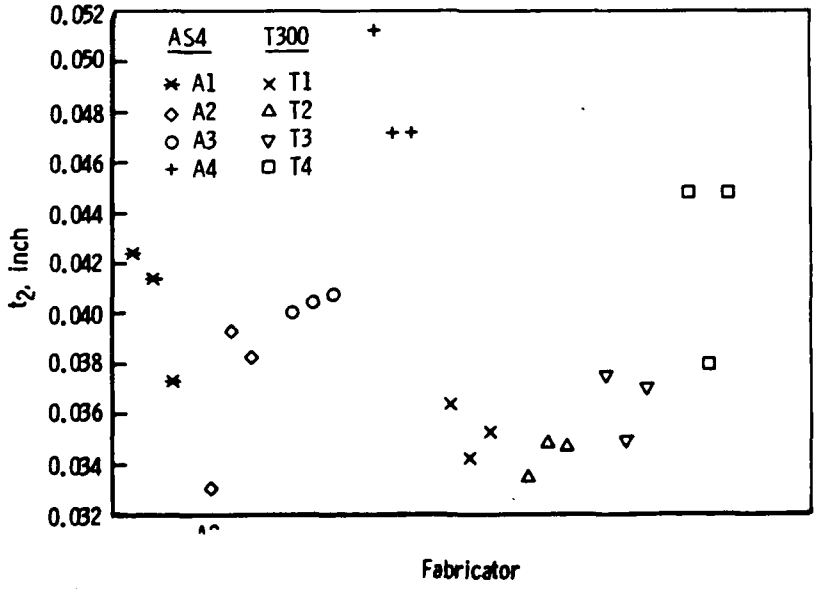

Figure 6. Thickness from QIA method, t_1, in inches for each tensile specimen fabricator.

In Figure 7, the tensile specimen thickness determined from the micrometer measurements, t_2, is plotted. Figure 7 is similar to Figure 6 in that it shows the variations within a particular fabricator and between the different fabricators.

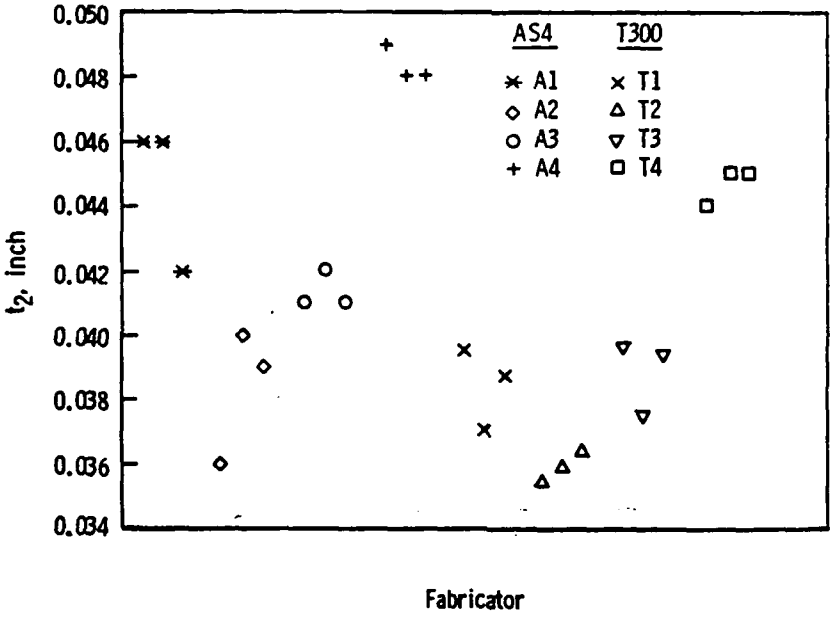

Figure 7. Thickness from micrometer method, t_2, in inches for each tensile specimen fabricator.

In Figure 8, the average thickness determined from the QIA method (t_1) versus the thickness from the micrometer measurements (t_2) is plotted. The average thickness QIA data has "spread" bars which represent the maximum and minimum thickness due to surface contour variation. In the micrometer method, the micrometer anvils span the peaks of the surface contours. As expected, the micrometer measurements are approximately equal to the QIA maximum thickness values which correspond to the upper limit of the "spread" bars. This agreement is demonstrated by noting that in Figure 8 the upper limit of the "spread" bars is reasonably close to the 45-degree linear equality dashed line. Hence, when these contours exist, conventional flat anvil micrometers provide only a maximum thickness value, and, because the surface contours vary within and between fabricators, the magnitude of the average or maximum thicknesses is not a constant. The magnitude of the micrometer thickness is on the average 2.2% greater than the average thickness determined using QIA techniques. (Note: The data for the statistical spread in the micrometer thickness measurements are not available, thus only the average value is plotted.)

The thickness and width are recorded for all fiber-reinforced composite mechanical test specimens. Hence, the improved accuracy of the QIA thickness measurement (t_1) versus the conventional micrometer thickness (t_2) becomes significant when the specimen's cross-sectional area is used for calculating the composite tensile strength.

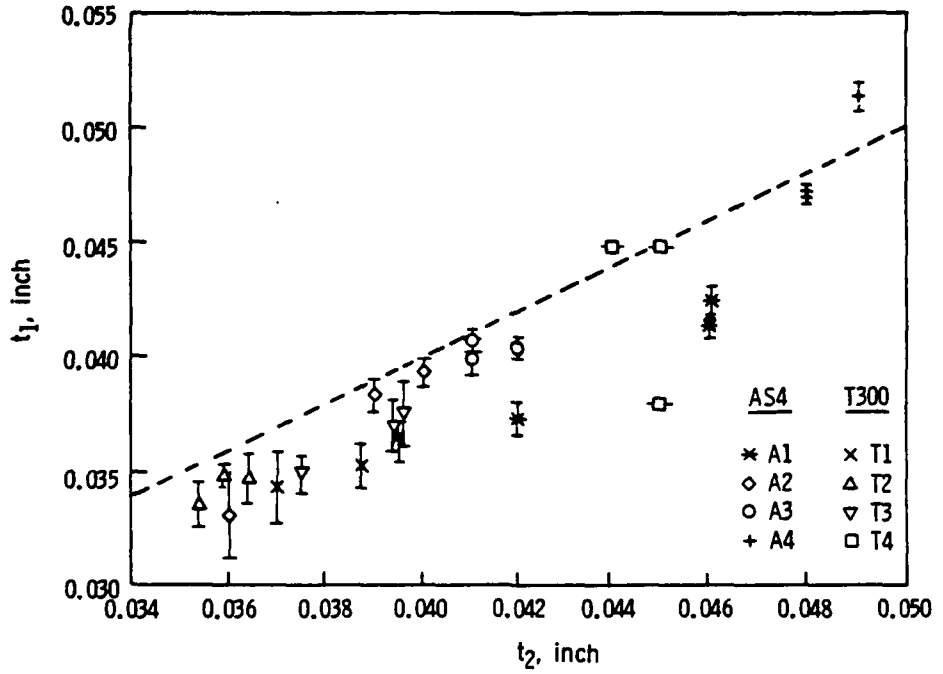

Figure 8. Average thickness from QIA method, t_1, in inches, versus thickness measured with micrometer, t_2, in inches for each tensile specimen.

Figure 9 shows the total thickness contour variation (Δt) determined from the QIA X-Y stage measuring technique for each tensile specimen. Although the general "shape" of the surface contour remains constant for six of the eight fabricators, the actual magnitude of the thickness variations Δt varies within all the fabricators except the T4 samples. Although T4 and A4 apparently use the same mold release film, A4 does have thickness variations present.

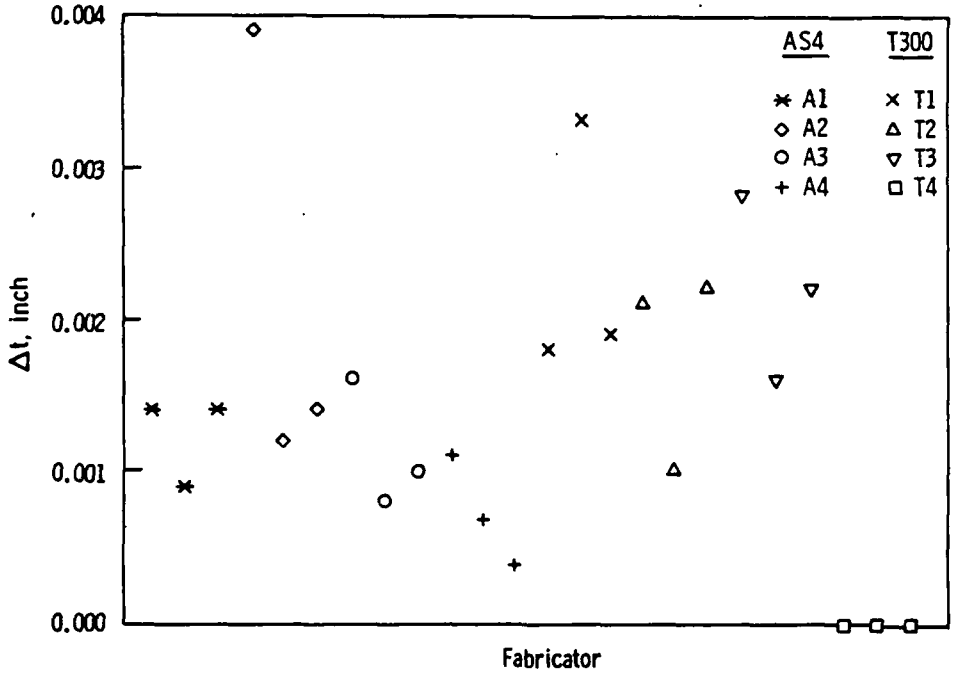

Figure 9. Maximum minus minimum thickness, Δt, in inches, for each tensile specimen fabricator.

Geometrical surface characteristics can influence adhesive bond strength or the durability of laminate coatings. For example, a scalloped-like surface, as seen in Figures 3c and 3e, could have both advantages and disadvantages. The advantage of the scalloped surface is that it provides a greater surface area for bonding and the geometry of the scalloping provides areas for entrapment of adhesive or coating materials, and, hence, may increase the joint strength or tab/grip performance. The disadvantage of this type of surface is the point-like peaks which could become areas of stress concentration when subjected to shear or the compressional forces. Specifying a release cloth or film type which would provide an optimum surface for a particular application should be introduced as a military specification.

QIA of Composite Tensile Specimen Cross Sections

The QIA data for each fabricator tabulated in Tables 1 through 8 designates A and B for each tabbed end of the particular tensile specimen. The data for A and B shows that the variation of the fiber area and the percent fiber area within a specific tensile specimen is small relative to specimen-to-specimen variations. The fiber area, A_{f1}, varied on the average ±1.5% between ends A and B of a particular tensile specimen. All specimens have zero or negligible void contents. The reproducibility of the QIA measurements had an average coefficient of variation of ±0.5%.

The method used in laminate lay-up and processing of unidirectional polymer fiber composite panels provides reasonable expectation that a small variation in fiber area content would exist from end-to-end of a 1-inch-wide axial tensile specimen. The low variation (±1.5%) of the fiber area measurements between the opposite ends of a particular tensile specimen provides evidence that the relative aspects of the QIA data is reliable; hence, can be used for comparing composite systems and/or individual samples and for determining if a correlation exists between fiber volume and the mechanical data.

The average percent fiber ($\%A_{f1}$) value for each fabricator is plotted in Figure 10 and illustrates the variation between fabricators. Quality assurance certification[2] from Hercules for the CFRP material, AS4/3501-6 prepreg tape, specifies a fractional fiber volume range from 56.8% to 72%. This range was calculated using the manufacturer's tolerances given for fiber density, areal weight of ply, and ply thickness. The CFRP laminates fabricators A1, A2, and A3 (see Figure 10) have average fractional fiber areas (equivalent to fractional fiber volumes)[4] in the range of 60% to 67%, as measured at MTL using QIA techniques. This data provides supporting evidence that the previously noted Hercules QIA specification tolerances used to calculate the percent fiber volume for the material in prepreg form are in agreement with the percent fiber volume QIA data obtained on the processed laminate. However, the A4 panels have 53% fiber. The A4 specimens are noticeably thicker than the other three manufacturers in this group with approximately the same fiber content, accounting for the lower percent fiber. The reason A4 specimens are thicker is probably due to the use of a mold release film rather than a mold release bleeder cloth which is used by the other three fabricators. On the average, QIA measurements indicate a 16% and 17% (T4: T300 and A4: AS4, respectively) fiber volume increase using a mold release bleeder cloth compared to a mold release film during processing. It is interesting to note that A4 and T4's percent fiber could not be predetermined by the Hercules method using fiber density, areal weight of ply, and ply thickness. Hercules did not stipulate a bleeder cloth type in order to stay within their percent fiber specification tolerance.

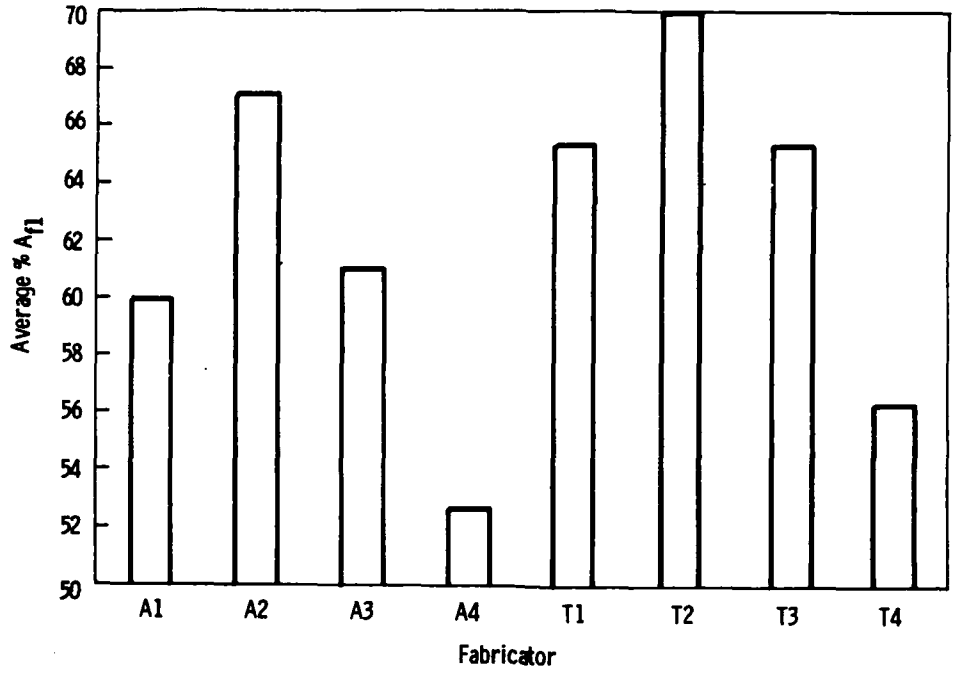

Figure 10. Average percent fiber area calculated from cross-sectional area, $\%A_{f1}$, for each fabricator.

In Figure 11, the percent fiber from direct QIA measurements ($\%A_{f2}$) versus the percent fiber calculated from the total cross-sectional fiber area ($\%A_{f1}$) is plotted for each tensile specimen. The two methods of acquiring %fiber area have subtle differences in the measurement procedure and represent different aspects of describing percentage fiber content (previously described in the QIA Methods and Measurement Section). The determination of $\%A_{f1}$ involves dividing the total fiber area (A_f) by a good approximation of the entire tensile specimen cross-sectional area (A_Q). The determination of $\%A_{f2}$ involved the direct measurement of total fiber area within each tensile specimen cross section. The procedure using the direct QIA method ($\%A_{f2}$) involved scanning an average of 75% of the total specimen cross-sectional area. The excluded 25% area was associated with the outer molded surface and edge regions. Hence, the $\%A_{f1}$ measurement, in principle, is more accurate than $\%A_{f2}$; however, it requires a considerably greater amount of time to acquire the data.

A source of error in the calculated percent fiber ($\%A_{f1}$) is the average cross-sectional sample area used because of surface contours. The error in the QIA direct measurement of percent fiber ($\%A_{f2}$) is generated by limitations in scanning the entire cross section which leads to variations in the percentage of actual cross section measured. It is assumed that these sources of error do not significantly effect the relative trends within or between manufacturers which were established in the comparative analysis of this data.

The spread of the points about the dashed 45-degree linear equality line in Figure 11 indicates reasonable agreement between these two approaches, thus providing a high degree of confidence in the direct percent fiber measurements ($\%A_{f2}$) of Method 2. The reasonable agreement in data further suggests that the two methods were equally suitable for obtaining

percent fiber area data. However, using Method 2 allows for substantial time savings and acceptable accuracy.

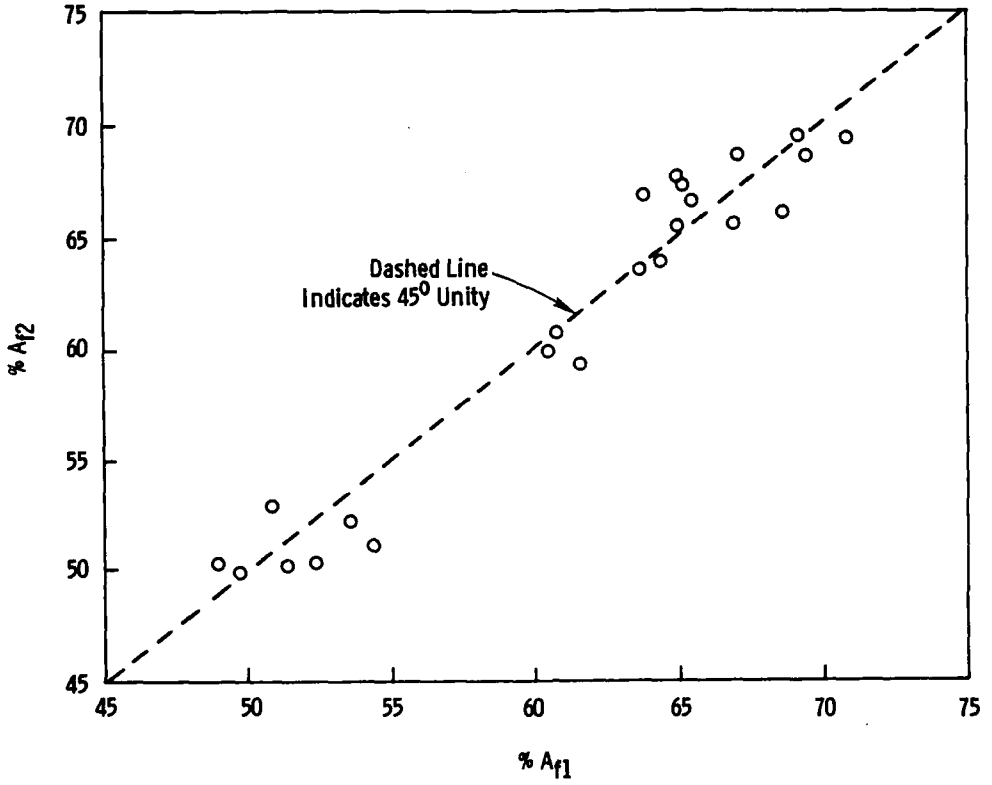

Figure 11. Percent fiber from direct QIA measurements, $\%A_{f2}$, versus percent fiber calculated from cross-sectional area, $\%A_{f1}$, for each tensile specimen.

The average percent fiber from direct QIA measurements ($\%A_{f2}$) for each tensile specimen versus the standard deviation of $\%A_{f2}$ is plotted in Figure 12. The standard deviation for the measurements of fractional fiber volume were of the order of ±10.7% for the AS4/3501-6 system and ±8.0% for the T300/934 system. The trend in this plot shows that composites with higher %fiber content had lower standard deviations, indicating a more densely packed fiber configuration within the cross section, and the converse is true for specimens with lower percent fiber content. Hence, the standard deviation is probably a good approximation of fiber uniformity within the scanned portion of the cross section. Again, all the $\%A_{f2}$ measurements were performed at the same Quantimet magnification, 435X, making it possible to compare the standard deviation variations between specimens.

Tables 10 and 11 list the average values for $(A_f/W)_1$ and $(A_f/W)_2$ for each fabricator. These tables show very good agreement between these two methods of determining fiber area per unit width. The $(A_f/W)_1$ values are considered the more accurate QIA measurement of the two methods since the entire specimen cross section is measured. However, the QIA measurement of percent fiber area can be achieved by only measuring approximately 75% of the cross-sectional area of the specimen, thus providing a time saving measurement advantage. The agreement between these methods provides greater confidence for using the $(A_f/W)_2$ percent fiber area method.

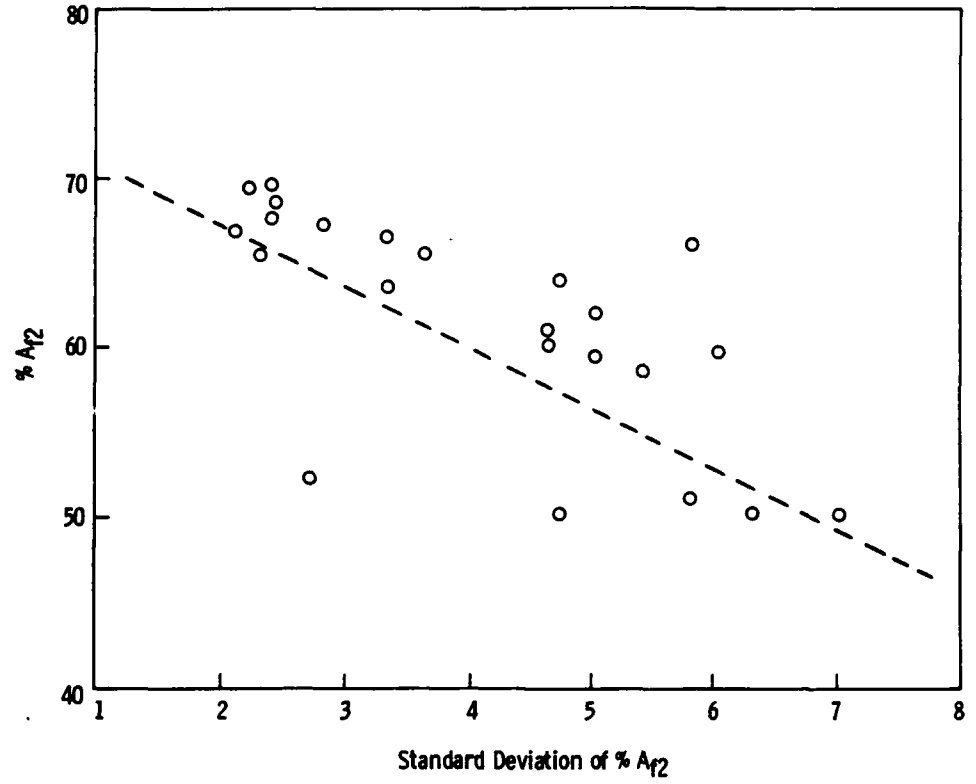

Figure 12. Percent fiber from QIA measurements, $\%A_{f2}$, versus the standard deviation of $\%A_{f2}$ for each tensile specimen.

Table 10. AVERAGE PARAMETER VALUES FOR AS4/3501-6 CARBON FIBER/RESIN COMPOSITE

MFG ID	$(A_f/W)_1$ sq. in./in.	$(A_f/W)_2$ sq. in./in.	$\%A_{f2}$	t_1 in.	A_{f1} sq. in.	W in.
A1	0.0243	0.0243	60.0	0.0405	0.0243	1.0010
A2	0.0243	0.0237	65.5	0.0362	0.0243	0.9992
A3	0.0246	0.0242	60.1	0.0403	0.0246	1.0021
A4	0.0253	0.0247	50.6	0.0488	0.0254	1.0042

Table 11. AVERAGE PARAMETER VALUES FOR T300/934 CARBON FIBER/RESIN COMPOSITE

MFG ID	$(A_f/W)_1$ sq. in./in.	$(A_f/W)_2$ sq. in./in.	$\%A_{f2}$	t_1 in.	A_{f1} sq. in.	W in.
T1	0.0231	0.0237	67.2	0.0353	0.0232	1.0062
T2	0.0241	0.0238	69.2	0.0344	0.0242	1.0065
T3	0.0239	0.0242	66.2	0.0366	0.0240	1.0060
T4	0.0238	0.0222	55.3	0.0402	0.0238	1.0033

The average fiber area per unit width, $(A_f/W)_1$, in inches squared per inch, is plotted in Figure 13 for each manufacturer. The $(A_f/W)_1$ is proposed as a good parameter for comparing fiber cross-sectional area variations between manufacturers since the width of the tensile specimens remained fairly constant; 1.0000 $\pm$0.0050 inches.

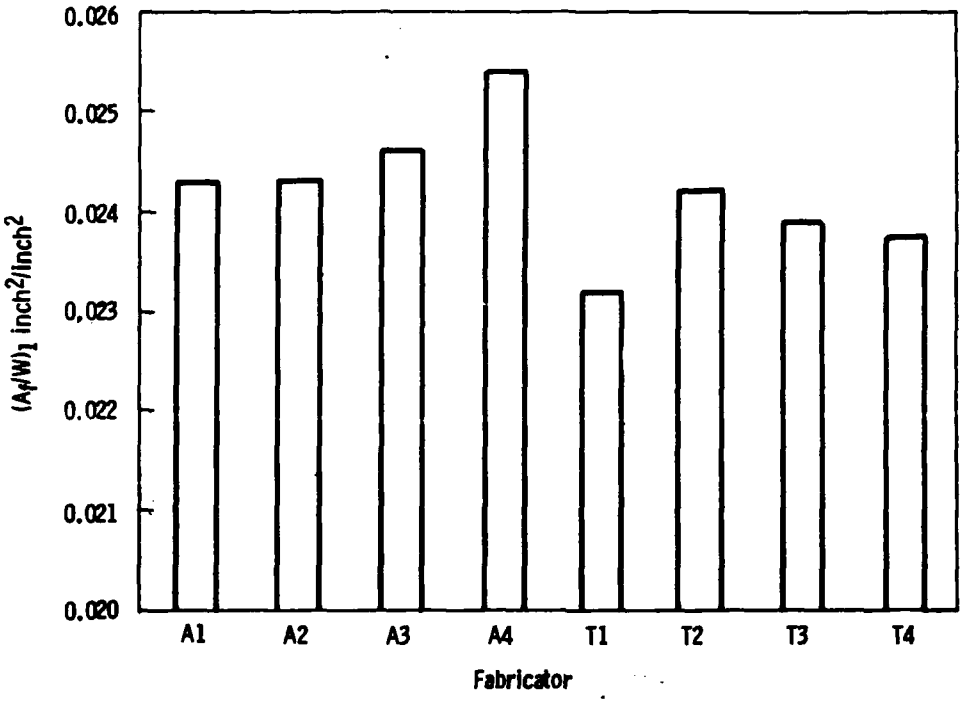

Figure 13. Average fiber area per unit width, $(A_f/W)_1$, in inches squared per inch, for each fabricator.

The concept of variations in fiber area or volume per unit width as a function of composite thickness was demonstrated by Whittenberger et al.[6] Whittenberger reported an inverse relationship between carbon fiber area or fiber volume and composite thickness. The suspected reason for this opposite trend demonstrated in his report is due to the composite width constraint imposed by the matched metal die mold used by Whittenberger. Materials analyzed in this MIL-HDBK-17 study were fabricated using an autoclave method, where composite width is unconstrained, allowing the fiber to spread out as the composite is compressed. This results in a decrease in thickness, which in turn causes a decrease in fiber area or volume per unit width.

The average fiber area per unit width, $(A_f/W)_1$, for the three tensile specimens in each manufacturing group versus the thickness determined from micrometer measurements (t_2) is plotted in Figure 14. Figure 14 indicates a definite trend of increasing fiber content with increasing thickness within each manufacturer in both fiber-resin systems. Lines are arbitrarily drawn connecting specimens of the same manufacturer for ease in visualizing the monotomic trends. However, the data is specific to a particular fabrication method and would not be suitable for fiber content comparison between fabricators. As shown, at a fiber area per unit width of 0.0227 in.^{2}/in. the micrometer thickness varies from 0.036 inches up to 0.048 inches depending on the fabricator; a 33% increase.

Although there are a limited number of points per fabricator, the monotomic increasing trend within each fabricator group appears to be consistent. It is suggested that a family of linear curves may exist with constant slope and curve intercept parameters which may be a

6. WHITTENBERGER, J. D. et al. *On Determination of Fibre Fraction in Continuous Fibre Composite Materials.* Journal of Materials Science Letters, v. 1, 1982.

function of other parameters such as resin content and/or processing variations. More data is needed to confirm this behavioral characteristic. However, establishing calibration quality control graphs of this type for each fabricator could prove useful in providing estimates in fiber content variations by monitoring composite thickness.

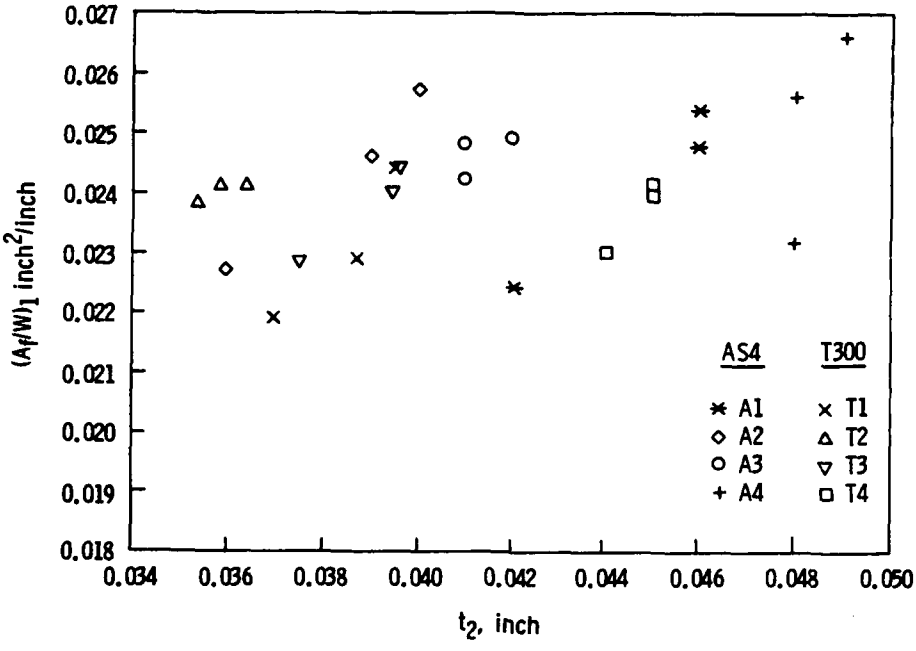

Figure 14. Average fiber area per unit width, $(A_f/W)_1$ for each tensile specimen, in inches squared per inch, versus thickness measured via micrometer, t_2, in inches, for each fabricator.

Quantitative image analysis is very effective in providing fiber volume uniformity, void sizes, and distributions. For determining bulk fiber volume of laminate panels, QIA is considered time consuming and costly in terms of sample preparation and measurement. Other techniques, such as wet chemistry and light intensity methods,[7,8] are probably sufficient for batch property data. However, QIA microstructural characterization of the individual test specimens (prior to or after testing) could be useful in the areas of mechanical property analysis and composite strength reproducibility. Such detailed information may translate into high reliability for the end user, and, hence, the cost justified. Also, one cannot overstress the use of microscopic examination for qualitative assessment of processed laminates as part of a routine quality assurance program.

CONCLUSIONS AND RECOMMENDATIONS

Surface contours due to mold release cloths are present in six of the eight fabricated panels. The surface contours varied between fabricators so the magnitudes of the average or

7. ASTM D 3171. *Standard Test Method for Fiber Content of Resin-Matrix Composites by Matrix Digestion.* American Society for Testing and Materials, 1976.
8. JOCK, C. P. *Quantitative Optical Microscopy Fiber Volume Methods for Composites.* Journal of Reinforced Plastics and Composites, v. 5, April 1986, p. 110.

maximum thicknesses are not constant. In some cases, a laminate surface contour generates an error of ±2.2% in the composite thickness values when using conventional flat anvil micrometers. Hence, when these molded surface contours exist, the flat anvil micrometers provide only a maximum thickness versus an average thickness. This could be a problem when calculating composite strength.

The QIA data shows that for each fabricator, the fiber content per unit width increases with increasing laminate micrometer thickness, indicating that the micrometer thickness could be used to monitor fiber content in the laminates, if calibration graphs specific to each fabrication process were generated.

On the average, QIA measurements indicate a 16% increase in fractional fiber volume using a mold release bleeder cloth compared to a mold release film during processing. The prepreg manufacturer's specification did not stipulate a mold release method or the possible influence it might have on the composite's fiber volume percent. Therefore, it is recommended that the prepreg manufacturer specify the mold release method used. It is further recommended that the imprints of the various types of mold release fabrics be characterized using qualitative or quantitative methods. The imprint characteristics or "fingerprints" could be cataloged and specified by fabricators. These could become important for composite testing and failure analysis, laminate coating, or bonding applications.

Quantitative image analysis is very effective in providing fiber volume uniformity, void sizes, and distributions. The end-to-end variation of the fiber area and the %fiber area within a specific specimen is small relative to specimen-to-specimen variations and the variability between fabricators. For all fabricators, the fiber area measurements vary on the average ±1.5% between ends A and B of a particular tensile specimen. These observations provide evidence that the relative aspects of the QIA data is reliable and can be used for comparing composite systems and/or individual samples and for determining if a relationship exists between fiber content and tensile strength. Actual composite material standards for optical QIA measurements do not exist, and, hence, the accuracy of the QIA cannot be determined. All specimens have zero or negligible void contents.

QIA can be used as a means of determining the fiber and void contents, surface conditions, and cross-sectional areas of individual mechanical test specimens prior to or after testing. Also, with continued advancements in the image processing and storage, microstructural data can be stored in the data base for future use. Coupling this microstructural data with the raw material specifications, fabrication parameters, and mechanical property data could prove to be very useful in understanding the behavior and improving the reliability of fiber-reinforced composite materials.

ACKNOWLEDGMENTS

The tensile specimens were provided by Mr. Robert Pasternak. We would like to thank Mr. Paul Doyle and Dr. James McCauley for their managerial support on this project.

APPENDIX A.1. ARTIFICIAL SPECIMEN SPECIFICATIONS

SPECIFICATIONS

DIMENSIONS: L: 75 mm W: 25 mm
L: 3 inches L: 1 inch

FEATURES:

SQUARE
50 x 50 ±2 μm
Area: 0.0025 mm^2

TRIANGLE
Base: 500 ±5 μm
Height: 435 ±5 μm

12 CIRCLES
Diameter: 103 ±2 μm
Total Area: 0.100 mm^2
Total Projection: 1.24 mm

108 BARS
2, 3, 6, ±0.8 μm Wide

ORDERING INFORMATION:

Order part number: 72164 Artificial Specimen Slide.

The Artificial Specimen slide is designed for checking Quantimet performance and for system calibration. It includes a series of high quality geometric features for use with transmitted or incident light microscopes.

APPENDIX A.2. MATERIALOGRAPHIC SAMPLE PREPARATION FOR QIA

SAMPLES: Carbon Fiber Reinforced Epoxy Composite Tensile Specimen

CUTTING:

Equipment: Struers' Accutom saw
Blade: Metal bond diamond, low concentration
Lubricant: Water
Blade Speed: 800 RPM
Feed Rate: 0.1 mm/minute
Sample Angle: 90 degrees to tensile load direction

MOUNTING:

Equipment: Buehler vacuum impregnation apparatus
Material: Struers' Epofix, room temperature, 8 hour epoxy

GRINDING:

Equipment: Struers' Planopol/Pedemax grinding machine
Materials: Struers' silicon carbide grinding papers
Lubricant: Tap water
Cleaning: Ultrasonically cleaned between each grinding step for 1 to 2 minutes in soapy tap water then rinsed in tap water.

Force, kp	Speed, rpm	Grit (μm)	Time, min*
2	300	500 (30)	sample thru
"	"	800 (21)	3 + 3
"	"	1000 (18)	3 + 3
"	"	1200 (15)	3 + 3
"	"	2400 (10)	3 + 3
"	"	4000 (5)	3 + 3

POLISHING:

Equipment: Struers' Planopol/Pedemax polishing machine
Materials: Struers' "DUR" silk cloth and diamond spray
Lubricant: Distilled water
Cleaning: Ultrasonically cleaned before and after polishing step for 1 to 2 minutes in soapy tap water. Rinsed in distilled water then ethanol and warm air dried.

Force, kp	Speed, rpm	Grit size	Time, min*
2	150	1 μm spray	3

*Time will vary with the total number of samples being prepared simultaneously. The above procedure was based on 3 samples. More samples will increase the grinding/polishing times. Also, these same carbon/epoxy samples without fiberglass composite tabs could probably half the allotted grinding time. Also, each additional 3 minute step per grit size requires a new grinding paper.

DISTRIBUTION LIST

No. of Copies	To
	Office of the Under Secretary of Defense for Research and Engineering, The Pentagon, Washington, DC 20301
1	ATTN: Mr. J. Persh
1	Dr. L. Young
1	Mr. K. R. Foster
	Commander, U.S. Army Laboratory Command, 2800 Powder Mill Road, Adelphi, MD 20783-1145
2	ATTN: AMSLC-IM-TL
1	AMSLC-TD
1	AMSLC-TD-A
1	AMSLC-PA
1	AMSLC-TP
1	AMSLC-CT
	Commander, Defense Technical Information Center, Cameron Station, Building 5, 5010 Duke Street, Alexandria, VA 22304-6145
2	ATTN: DTIC-FDAC
1	National Technical Information Service, 5285 Port Royal Road, Springfield, VA 22161
	Director, Defense Advanced Research Projects Agency, 1400 Wilson Boulevard, Arlington, VA 22209
1	ATTN: Dr. P. Parrish
1	Dr. B. Wilcox
1	Dr. K. Hardmann-Rhyne
	Battelle Columbus Laboratories, Metals and Ceramics Information Center, 505 King Avenue, Columbus, OH 43201
1	ATTN: Mr. W. Duckworth
1	Dr. D. Niesz
	Department of the Army, Office of the Assistant Secretary of the Army (RDA), Washington, DC 20310
1	ATTN: Dr. J. G. Prather, Dep for Sci & Tech
1	Dr. J. R. Sculley, SARD
	Deputy Chief of Staff, Research, Development, and Acquisition, Headquarters, Department of the Army, Washington, DC 20310
1	ATTN: DAMA-ZE, Mr. C. M. Church
	Commander, U.S. Army Research and Development Office, Chief Research and Development, Washington, DC 20315
1	ATTN: Physical and Engineering Sciences Division
	Commander, Army Research Office, P.O. Box 12211, Research Triangle Park, NC 27709-2211
1	ATTN: Information Processing Office
1	Dr. J. Hurt
1	Dr. A. Crowson
1	Dr. R. Reeber
1	Dr. R. Shaw
	Commander, U.S. Army Materiel Command, 5001 Eisenhower Avenue, Alexandria, VA 22333
1	ATTN: AMCQA-EQ, Mr. H. L. Light
1	AMCQA, Mr. S. J. Lorber
	Commander, U.S. Army Materiel Systems Analysis Activity, Aberdeen Proving Ground, MD 21005
1	ATTN: AMXSY-MP, H. Cohen
	Commander, U.S. Army Night Vision Electro-Optics Laboratory, Fort Belvoir, VA 22060
1	ATTN: DELNV-S, Mr. P. Travesky
1	DELNV-L-D, Dr. R. Buser
1	DELNV-D, Dr. L. Cameron
	Commander, Harry Diamond Laboratories, 2800 Powder Mill Road, Adelphi, MD 20783
1	ATTN: Technical Information Office
1	SLCHD-RAE
	Director, U.S. Army Research & Technology Labs, Ames Research Center, Moffet Field, CA 94035
1	ATTN: DAVDL-D, Dr. R. Carlson
1	DAVDL-AL-D, Dr. I. C. Statler, MS215-1, Aeromechanics Laboratory
	Commander, U.S. Army Missile Command, Redstone Scientific Information Center, Redstone Arsenal, AL 35898-5241
1	ATTN: AMSMI-RD-CS-R/Doc
1	AMSMI-R, Dr. W. C. McCorkle
	Commander, U.S. Army Aviation Systems Command, P.O. Box 209, St. Louis, MO 63120-1798
1	ATTN: AMSAV-NS, Mr. M. L. Bauccio
1	Technical Library
	Commander, U.S. Army Natick Research, Development, and Engineering Center, Natick, MA 01760
1	ATTN: Technical Library
1	Dr. J. A. Sousa
1	Dr. R. J. Byrne
1	Dr. R. Lewis
	Commander, U.S. Army Satellite Communications Agency, Fort Monmouth, NJ 07703
1	ATTN: Technical Document Center
	Commander, U.S. Army Science and Technology Center Far East Office, APO San Francisco, CA 96328
1	ATTN: Terry L. McAfee
	Commander, U.S. Army Communications and Electronics Command, Fort Monmouth, NJ 07703
1	ATTN: AMSEL-TDD, Mr. T. A. Pfeiffer, Technical Dir.
	Director, Electronic Technology and Devices Lab, Fort Monmouth, NJ 07703
1	ATTN: DELET-D, Dr. C. G. Thornton
	Commander, U.S. Army Tank-Automotive Command, Warren, MI 48397-5000
1	ATTN: Dr. W. Bryzik
1	D. Rose
1	AMSTA-RKA
1	AMSTA-UL, Technical Library
1	AMSTA-R
1	AMSTA-NS, Dr. H. H. Dobbs
	Commander, U.S. Army Armament, Munitions and Chemical Command, Dover, NJ 07801
1	ATTN: Mr. J. Lannon
1	Mr. H. E. Pebly, Jr., PLASTEC, Director
1	Technical Library
1	Dr. T. Davidson
1	Dr. B. Ebihara
	Commander, U.S. Army Armament, Munitions and Chemical Command, Rock Island, IL 61299
1	ATTN: Technical Library
	Commander, U.S. Army Chemical Research, Development and Engineering Center, Aberdeen Proving Ground, MD 21010-5423
1	ATTN: SMCCR-TD, Mr. J. Vervier
	U.S. Army Corps of Engineers, Construction Engineering Research Lab, P.O. Box 4005, Champaign, IL 61820
1	ATTN: Dr. Robert Quattrone
	Commander, U.S. Army Belvoir RD&E Center, Fort Belvoir, VA 22060-5606
1	ATTN: STRBE-FS, Mr. W. McGovern, Fuel & Wtr Sup Div
1	AMDME-V, Mr. E. York
1	STRBE-ZTS, Dr. K. H. Steinbach, Office of the Chief Scientist
1	AMDME-ZT, Mr. T. W. Lovelace, Tech Dir
1	Mr. M. Lepera
	Director, U.S. Army Ballistic Research Laboratory, Aberdeen Proving Ground, MD 21005
1	ATTN: SLCBR-BLT, Dr. A. M. Dietrich
1	SLCBR-BLF, Dr. A. Niller
	Commander, Rock Island Arsenal, Rock Island, IL 61299
1	ATTN: SARRI-EN

No. of Copies	To
	Director, U.S. Army Industrial Base Engineering Activity, Rock Island, IL 61299
1	ATTN: AMXIB-MT, Mr. G. B. Ney
	Commander, U.S. Army Chemical Research, Development, and Engineering Center, Aberdeen Proving Ground, MD 21010-5423
1	ATTN: AMSMC-CLD(A), Dr. B. Richardson
	Commander, U.S. Army Test and Evaluation Command, Aberdeen Proving Ground, MD 21005
1	ATTN: AMSTE-ME
1	AMSTE-TD, Mr. H. J. Peters
	Commander, U.S. Army Foreign Science and Technology Center, 220 7th Street, N.E., Charlottesville, VA 22901
1	ATTN: Military Tech
1	Mr. J. Crider
1	Ms. P. Durrer
1	Mr. P. Greenbawm
	Chief, Benet Weapons Laboratory, Watervliet, NY 12189
1	ATTN: AMDAR-LCB-TL
1	Dr. G. D'Andrea
1	AMDAR-LCB, Dr. F. Sautter
	Commander, U.S. Army Aviation Systems Command, Aviation Research and Technology Activity, Aviation Applied Technology Directorate, Fort Eustis, VA 23604-5577
1	ATTN: SAVDL-E-MOS
	Commander, U.S. Army Engineer Waterways Experiment Station, Vicksburg, MS 39180
1	ATTN: Research Center Library
	Project Manager, Munitions Production Base, Modernization and Expansion, Dover, NJ 07801
1	ATTN: AMCPM-PBM-P
	Technical Director, Human Engineering Laboratories, Aberdeen Proving Ground, MD 21005-5001
1	ATTN: SLCHE-D, Dr. J. D. Weisz
	Chief of Naval Research Arlington, VA 22217
1	ATTN: Code 471
1	Dr. A. Diness
1	Dr. R. Pohanka
	Naval Research Laboratory, Washington, DC 20375
1	ATTN: Code 5830
	Headquarters, Naval Air Systems Command, Washington, DC 20360
1	ATTN: Code 5203
	Headquarters, Naval Sea Systems Command, 1941 Jefferson Davis Highway, Arlington, VA 22376
1	ATTN: Code 035
	Headquarters, Naval Electronics Systems Command, Washington, DC 20360
1	ATTN: Code 504
	Commander, Naval Ordnance Station, Louisville, KY 40214
1	ATTN: Code 50D
1	Director, Naval Industrial Resources Support Activity, Building 75-2, Room 209, Naval Base, Philadelphia, PA 19112-5078
	Commander, Weapons Center, China Lake CA 93555
1	ATTN: Mr. F. Markarian
	Commander, U.S. Air Force Wright Aeronautical Labs, Wright-Patterson Air Force Base, OH 45433
1	ATTN: Dr. N. Tallan
1	Dr. H. Graham
1	Dr. R. Ruh
1	Aero Propulsion Labs, Mr. R. Marsh
1	Dr. H. M. Burte
1	AFWAL/MLLP, Mr. D. Forney
1	AFML/MLLM, Mr. H. L. Gegel
1	AFSC/MLLM, Dr. A. Katz

No. of Copies	To
	Commander, Air Force Armament Center, Eglin Air Force Base, FL 32542
1	ATTN: Technical Library
	National Aeronautics and Space Administration, Lewis Research Center, 21000 Brookpark Road, Cleveland, OH 44135
1	ATTN: J. Accurio, USAMRDL
1	Dr. H. B. Probst, MS 49-1
1	Dr. S. Dutta
1	NASA - Scientific and Technical Information Facility, P.O. Box 8757, Baltimore/Washington International Airport, Maryland 21240
	NASA - Langley Research Center, Hampton, VA 23665
1	ATTN: Mr. J. Buckley, MS 387
1	Dr. J. Heyman, MS 231
1	Dr. Wolf Elber, Dir., Aerostructures Directorate, MS 266
	Commander, White Sands Missile Range, Electronic Warfare Laboratory, OMEW, ERADCOM, White Sands, NM 88002
1	ATTN: Mr. Thomas Reader, AMSEL-WLM-ME
	Department of Energy, Division of Transportation, 20 Massachusetts Avenue, N.W., Washington, DC 20545
1	ATTN: Dr. R. J. Gottschall, ER-131, GTN
1	Mechanical Properties Data Center, Belfour Stulen Inc., 13917 W. Bay Shore Drive, Traverse City, MI 49684
	National Institute of Standards and Technology, Washington, DC 20234
1	ATTN: E. S. Etz, Bldg. 222, Rm A-121
1	D. L. Hunston, Bldg. 224, Rm A-209
1	Dr. D. H. Reneker, Dep. Dir., Ctr for Matl's Sci.
1	Dr. Lyle Schwartz
1	Dr. Stephen Hsu
1	Dr. Allan Draggoo
	U.S. Bureau of Mines, Mineral Resources Technology, 2401 E. Street, N.W., Washington, DC 20241
1	ATTN: Mr. M. A. Schwartz
	National Institute of Standards and Technology, Gaithersburgh, MD 20899
1	ATTN: Dr. S. Wiederhorn
	National Research Council, National Materials Advisory Board, 2101 Constitution Avenue, Washington, DC 20418
1	ATTN: Dr. K. Zwilsky
1	D. Groves
1	J. Lane
	National Science Foundation, Materials Division, 1800 G Street, N.W., Washington, DC 20006
1	ATTN: Dr. L. Toth
1	Dr. J. Hurt
	AVCO Corporation, Applied Technology Division, Lowell Industrial Park, Lowell, MA 01887
1	ATTN: Dr. T. Vasilos
	Case Western Reserve University, Department of Metallurgy, Cleveland, OH 60605
1	ATTN: Prof. A. H. Heuer
	Defence Research Establishment Pacific, FMO, Victoria, B.C., VOS IBO, Canada
1	ATTN: R. D. Barer
	Ford Motor Company, Turbine Research Department, 20000 Rotunda Drive, Dearborn, MI 48124
1	ATTN: T. Whelan
	Ford Motor Company, P.O. Box 2053, Dearborn, MI 48121
1	ATTN: Dr. D. Compton, Vice President Research
	General Electric Company, Research and Development Center, Box 8, Schenectady, NY 12345
1	ATTN: Dr. R. J. Charles
1	Dr. C. D. Greskovich
1	Dr. S. Prochazka

No. of Copies	To
	GTE Sylvania, Waltham Research Center, 40 Sylvania Road, Waltham, MA 02154
1	ATTN: Dr. W. H. Rhodes
	Martin Marietta Laboratories, 1450 South Rolling Road, Baltimore, MD 21227
1	ATTN: Dr. J. Venables
	Massachusetts Institute of Technology, Department of Metallurgy and Materials Science, Cambridge, MA 02139
1	ATTN: Prof. R. L. Coble
1	Prof. H. K. Bowen
1	Prof. W. D. Kingery
1	Prof. J. Vander Sande
	Midwest Research Institute, 425 Volker Boulevard, Kansas City, MO 64110
1	ATTN: Mr. G. W. Gross, Head, Physics Station
	Pennsylvania State University, Materials Research Laboratory, Materials Science Department, University Park, PA 16802
1	ATTN: Prof. R. Roy
1	Prof. R. E. Newnham
1	Prof. R. E. Tressler
1	Dr. C. Pantano
1	Mr. C. O. Ruud
	State University of New York at Albany, Department of Physics, Albany, NY 12222
1	ATTN: Prof. W. A. Lanford
	State University of New York at Stony Brook, Department of Materials Science, Long Island, NY 11790
1	ATTN: Prof. F. F. Y. Wang
	Stanford Research International, 333 Ravenswood Avenue, Menlo Park, CA 94025d
1	ATTN: Dr. P. Jorgensen
1	Dr. D. Rowcliffe
	United Technologies Research Center, East Hartford, CT 06108
1	ATTN: Dr. J. Brennan
1	Dr. K. Prewo
	University of California, Lawrence Livermore Laboratory, P.O. Box 808, Livermore, CA 94550
1	ATTN: Mr. R. Landingham
1	Dr. C. F. Cline
1	Dr. J. Birch Holt
	University of Florida, Department of Materials Science and Engineering, Gainevisille, FL 32611
1	ATTN: Dr. L. Hench
	University of Washington, Ceramic Engineering Division, FB-10, Seattle, WA 98195
1	ATTN: Prof. R. Bradt
	Westinghouse Electric Corporation, Research Laboratories, Pittsburgh, PA 15235
1	ATTN: Dr. R. J. Bratton
	Rensselaer Polytechnic Institute, Department of Materials Engineering, Troy, NY 12181
1	ATTN: R. J. Diefendorf
	Oak Ridge National Laboratory, P.O. Box X Oak Ridge, TN 37830
1	ATTN: P. F. Becher
1	V. J. Tennery
1	R. Johnson
	Sandia Laboratories, Albuquerque, NM 87185
1	ATTN: Dr. F. Gerstle, Div 5814
	The John Hopkins University, Department of Civil Engineering/ Materials Science and Engineering, Baltimore, MD 28218
1	ATTN: Dr. R. E. Green, Jr.

No. of Copies	To
1	Director, Office of Science and Technology Policy, Old Executive Office Building, Washington, DC 20223
	Subcommittee on Science, 2319 Rayburn House Office Building, Washington, DC 20515
1	ATTN: Mr. P. C. Maxwell
	Aerospace Corporation, Materials Science Laboratory, 2350 East El Segundo Boulevard, El Segundo, CA 90245
1	ATTN: Dr. L. R. McCreight
	IBM Corporation, Thomas B. Watson Research Center, Yorkstown Heights, NY 10598
1	ATTN: Dr. G. Onoda
	Corning Glass Works, Research and Development Division, Corning, NY 14830
1	ATTN: Dr. W. R. Prindle
	3M Company, New Products Department, 218-35-04, 3M Center, St. Paul, MN 55144
1	ATTN: R. E. Richards
	Technology Strategies, Inc., 10722 Shingle Oak Ct., Burke, VA 22015
1	ATTN: Dr. E. C. Van Reuth
	Rutgers University, Center for Ceramics, Rm A274, P.O. Box 909, Piscataway, NJ 08854
1	ATTN: Prof. J. B. Wachtman, Jr., Director
	Syracuse University, 304 Administration Building, Syracuse, NY 13210
1	ATTN: Dr. V. Weiss
	Lehigh University, Materials Research Center #32, Bethlehem, PA 18015
1	ATTN: Dr. D. M. Smyth
	Alfred University, New York State College of Ceramics, Alfred, NY 14802
1	ATTN: Dr. R. L. Snyder
	Alfred University, Center for Advanced Ceramic Technology, Alfred, NY 14802
1	ATTN: R. M. Spriggs
	University of California, Center for Advanced Materials, D58, Hildebrand Hall, Berkeley, CA 94720
1	ATTN: Prof. G. Somorjai
	Boeing Aerospace Company, 11029 Southeast 291, Auburn, MA 98002
1	ATTN: W. E. Strobelt
	University of California, Materials Science and Mineral Engineering, Heart Mining Building, Rm 284, Berkeley, CA 94720
1	ATTN: Prof. G. Thomas
	Director, U.S. Army Materials Technology Laboratory, Watertown, MA 02172-0001
2	ATTN: SLCMT-TML
2	Authors

U.S. Army Materials Technology Laboratory
Watertown, Massachusetts 02172-0001
QUANTITATIVE MICROSTRUCTURAL ANALYSIS OF UNIDIRECTIONAL CARBON FIBER REINFORCED POLYMER COMPOSITES, PART 1: MICROSTRUCTURAL CHARACTERIZATION OF COMPOSITE CROSS SECTION -
John J. Ricca and Rebecca M. Jurta

Technical Report MTL TR 90-1, January 1990, 34 pp-illus-tables, D/A Project: 1L162105.AH84

AD__________
UNCLASSIFIED
UNLIMITED DISTRIBUTION

Key Words

Carbon fiber
Polymer composite
Laminates

Individual axial tensile specimens of AS4/3501-6 and T300/934 unidirectional carbon fiber reinforced polymer composite laminate systems are characterized microstructurally. Fiber volume, fractional fiber volume, fiber uniformity, void volume, and variations in laminate thickness are acquired using automated quantitative image analysis (QIA). The sample preparation methods and QIA system procedures are fully explained. The problems in determining average or batch fiber contents in composite laminates using current methods are discussed. Possible problems in using micrometer thickness data in fiber content calculations are discussed when variations in specimen thickness due to surface contours are present. Variations in microstructure exhibited within a single fabricating company, between several fabricating companies, and between two different fiber-resin systems are demonstrated. Overall, QIA was determined to be a precise means of determining fiber and void contents and uniformity in individual test specimens prior to or after mechanical testing.

U.S. Army Materials Technology Laboratory
Watertown, Massachusetts 02172-0001
QUANTITATIVE MICROSTRUCTURAL ANALYSIS OF UNIDIRECTIONAL CARBON FIBER REINFORCED POLYMER COMPOSITES, PART 1: MICROSTRUCTURAL CHARACTERIZATION OF COMPOSITE CROSS SECTION -
John J. Ricca and Rebecca M. Jurta

Technical Report MTL TR 90-1, January 1990, 34 pp-illus-tables, D/A Project: 1L162105.AH84

AD__________
UNCLASSIFIED
UNLIMITED DISTRIBUTION

Key Words

Carbon fiber
Polymer composite
Laminates

Individual axial tensile specimens of AS4/3501-6 and T300/934 unidirectional carbon fiber reinforced polymer composite laminate systems are characterized microstructurally. Fiber volume, fractional fiber volume, fiber uniformity, void volume, and variations in laminate thickness are acquired using automated quantitative image analysis (QIA). The sample preparation methods and QIA system procedures are fully explained. The problems in determining average or batch fiber contents in composite laminates using current methods are discussed. Possible problems in using micrometer thickness data in fiber content calculations are discussed when variations in specimen thickness due to surface contours are present. Variations in microstructure exhibited within a single fabricating company, between several fabricating companies, and between two different fiber-resin systems are demonstrated. Overall, QIA was determined to be a precise means of determining fiber and void contents and uniformity in individual test specimens prior to or after mechanical testing.

U.S. Army Materials Technology Laboratory
Watertown, Massachusetts 02172-0001
QUANTITATIVE MICROSTRUCTURAL ANALYSIS OF UNIDIRECTIONAL CARBON FIBER REINFORCED POLYMER COMPOSITES, PART 1: MICROSTRUCTURAL CHARACTERIZATION OF COMPOSITE CROSS SECTION -
John J. Ricca and Rebecca M. Jurta

Technical Report MTL TR 90-1, January 1990, 34 pp-illus-tables, D/A Project: 1L162105.AH84

AD__________
UNCLASSIFIED
UNLIMITED DISTRIBUTION

Key Words

Carbon fiber
Polymer composite
Laminates

Individual axial tensile specimens of AS4/3501-6 and T300/934 unidirectional carbon fiber reinforced polymer composite laminate systems are characterized microstructurally. Fiber volume, fractional fiber volume, fiber uniformity, void volume, and variations in laminate thickness are acquired using automated quantitative image analysis (QIA). The sample preparation methods and QIA system procedures are fully explained. The problems in determining average or batch fiber contents in composite laminates using current methods are discussed. Possible problems in using micrometer thickness data in fiber content calculations are discussed when variations in specimen thickness due to surface contours are present. Variations in microstructure exhibited within a single fabricating company, between several fabricating companies, and between two different fiber-resin systems are demonstrated. Overall, QIA was determined to be a precise means of determining fiber and void contents and uniformity in individual test specimens prior to or after mechanical testing.

U.S. Army Materials Technology Laboratory
Watertown, Massachusetts 02172-0001
QUANTITATIVE MICROSTRUCTURAL ANALYSIS OF UNIDIRECTIONAL CARBON FIBER REINFORCED POLYMER COMPOSITES, PART 1: MICROSTRUCTURAL CHARACTERIZATION OF COMPOSITE CROSS SECTION -
John J. Ricca and Rebecca M. Jurta

Technical Report MTL TR 90-1, January 1990, 34 pp-illus-tables, D/A Project: 1L162105.AH84

AD__________
UNCLASSIFIED
UNLIMITED DISTRIBUTION

Key Words

Carbon fiber
Polymer composite
Laminates

Individual axial tensile specimens of AS4/3501-6 and T300/934 unidirectional carbon fiber reinforced polymer composite laminate systems are characterized microstructurally. Fiber volume, fractional fiber volume, fiber uniformity, void volume, and variations in laminate thickness are acquired using automated quantitative image analysis (QIA). The sample preparation methods and QIA system procedures are fully explained. The problems in determining average or batch fiber contents in composite laminates using current methods are discussed. Possible problems in using micrometer thickness data in fiber content calculations are discussed when variations in specimen thickness due to surface contours are present. Variations in microstructure exhibited within a single fabricating company, between several fabricating companies, and between two different fiber-resin systems are demonstrated. Overall, QIA was determined to be a precise means of determining fiber and void contents and uniformity in individual test specimens prior to or after mechanical testing.